

Two improved algorithms for sparse generalized canonical correlation analysis*

Kuo-Yue Li^a, Qi-Ye Zhang^{a,*}, Yong-Han Sun^a

^a*School of Mathematical Science, Beihang University, Beijing 102206, P. R. China*

Abstract

Regularized generalized canonical correlation analysis (RGCCA) is a generalization of regularized canonical correlation analysis to three or more sets of variables, which is a component-based approach aiming to study the relationships between several sets of variables. Sparse generalized canonical correlation analysis (SGCCA) (proposed in Tenenhaus et al. (2014)), combines RGCCA with an ℓ_1 -penalty, in which blocks are not necessarily fully connected, makes SGCCA a flexible method for analyzing a wide variety of practical problems, such as biology, chemistry, sensory analysis, marketing, food research, etc. In Tenenhaus et al. (2014), an iterative algorithm for SGCCA was designed based on the solution to the subproblem (LM-P1 for short) of maximizing a linear function on the intersection of an ℓ_1 -norm ball and a unit ℓ_2 -norm sphere proposed in Witten et al. (2009). However, the solution to the subproblem (LM-P1) proposed in Witten et al. (2009) is not correct, which may become the reason that the iterative algorithm for SGCCA is slow and not always convergent. For this, we first characterize the solution to the subproblem LM-P1, and the subproblems LM-P2 and LM-P3, which maximize a linear function on the intersection of an ℓ_1 -norm sphere and a unit ℓ_2 -norm sphere, and an ℓ_1 -norm ball and a unit ℓ_2 -norm sphere, respectively. Then we provide more efficient block coordinate descent (BCD) algorithms for SGCCA and its two variants, called SGCCA-BCD1, SGCCA-BCD2 and SGCCA-BCD3, corresponding to the subproblems LM-

*This work was supported in part by the National Natural Science Foundation of China under grant numbers 61172060 and 62133001.

*Corresponding author

Email addresses: sy2109121@buaa.edu.cn (Kuo-Yue Li), zhangqiye@buaa.edu.cn (Qi-Ye Zhang), 18222247343@163.com (Yong-Han Sun)

P1, LM-P2 and LM-P3, respectively, prove that they all globally converge to their stationary points. We further propose gradient projected (GP) methods for SGCCA and its two variants when using the Horst scheme, called SGCCA-GP1, SGCCA-GP2 and SGCCA-GP3, corresponding to the sub-problems LM-P1, LM-P2 and LM-P3, respectively, and prove that they all globally converge to their critical points. Finally, we conduct two numerical experiments in R environment to evaluate the performance of our proposed BCD algorithms and GP methods for SGCCA and its variants. Simulation results show that compared to the original SGCCA algorithm with the same solution quality, our BCD algorithms speed up at least 10%, 13%, 59% on the artificial data and 23%, 13%, 59% on the real glioma data using the Horst, centroid and factorial schemes, respectively; however, our GP methods improve the solution quality with a little bit lost efficiency on the artificial data, improve the solution quality and efficiency on the real glioma data using the Horst scheme.

Keywords: Sparse generalized canonical correlation analysis, block coordinate descent algorithm, linear function maximization, projection onto an intersection of an ℓ_1 -norm ball (sphere) and an unit ℓ_2 -norm ball (sphere), gradient projected method

1. Introduction

A challenging problem in multivariate statistics has been studying the relationship between several sets of variables measured on the same set of individuals, often called “learning from multimodal data”, “data integration” or “multi-block data analysis”. It has been widely applied in biology, chemistry, sensory analysis, marketing, food research, etc., to identify the variables in each block, in which these variables are active in relation to other blocks.

Hotelling et al. Hotelling (1936) put forward canonical correlation analysis (CCA) in 1936 to study the linear correlation between two groups of variables. Considering two sets of variates $\mathbf{x} = (x_1, x_2, \dots, x_p)^T$ and $\mathbf{y} = (y_1, y_2, \dots, y_q)^T$, let us denote the covariances, in the sense of expectations of products, by $V(\mathbf{x}) = \Sigma_{11}(> 0)$, $V(\mathbf{y}) = \Sigma_{22}(> 0)$ and $\text{Cov}(\mathbf{x}, \mathbf{y}) = \Sigma_{12}$. In order to reflect the correlation between the two sets of variables to the greatest extent, \mathbf{x} and \mathbf{y} are compressed as linear functions into univariate $u = \mathbf{a}^T \mathbf{x}$ and $v = \mathbf{b}^T \mathbf{y}$, where \mathbf{a} , \mathbf{b} are non-zero constant vectors. Then one

can get two linear functions $u_1 = \mathbf{a}_1^T \mathbf{x}$, $v_1 = \mathbf{b}_1^T \mathbf{y}$ by solving the following optimization problem:

$$\begin{aligned} \max_{\mathbf{a}, \mathbf{b}} \rho(u, v) &= \frac{\mathbf{a}^T \Sigma_{12} \mathbf{b}}{\sqrt{\mathbf{a}^T \Sigma_{11} \mathbf{a}} \sqrt{\mathbf{b}^T \Sigma_{22} \mathbf{b}}} \\ \text{s.t. } \mathbf{a}^T \Sigma_{11} \mathbf{a} &= 1 \\ \mathbf{b}^T \Sigma_{22} \mathbf{b} &= 1 \end{aligned} \tag{1.1}$$

where u_1 and v_1 are the first pair of canonical variables. If the first part is not enough, the second pair of typical variables u_2, v_2 can be found in the remaining correlation. In general, the i th pair of canonical variables $u_i = \mathbf{a}^T \mathbf{x}$, $v_i = \mathbf{b}^T \mathbf{y}$ are obtained by maximizing $\rho(u_i, v_i) = \rho(\mathbf{a}^T \mathbf{x}, \mathbf{b}^T \mathbf{y}) = \frac{\mathbf{a}^T \Sigma_{12} \mathbf{b}}{\sqrt{\mathbf{a}^T \Sigma_{11} \mathbf{a}} \sqrt{\mathbf{b}^T \Sigma_{22} \mathbf{b}}}$ when $\mathbf{a}^T \Sigma_{11} \mathbf{a} = 1$, $\mathbf{b}^T \Sigma_{22} \mathbf{b} = 1$, $\mathbf{a}^T \Sigma_{11} \mathbf{a}_k = 0$, $\mathbf{b}^T \Sigma_{22} \mathbf{b}_k = 0$, $k = 1, 2, \dots, i - 1$. Horst et al. Horst (1961) used Hotelling's method to solve the problem of determining the linear function of two groups of variables in order to maximize the correlation between the two functions. They gave a more efficient computational solution for the case of two sets of variables, and put forward a generalized solution for any number of sets. Kettenring Kettenring (1971) extended the classical two-set theory of CCA to three or more sets, and measured the strength of the relationship using a generalized canonical correlation coefficients, such as the sum of correlations method (SUMCOR), the maximum variance method (MAXVAR), the sum of squared correlations method (SSQCOR), the minimum variance method (MINVAR), the generalized variance method (GENVAR), etc. The objective functions of these methods are correlation coefficient or covariance function, or the combination of correlation coefficient and covariance. The model seems complicated, but there are certain similarities. For example, each of these three procedures for SUMCOR, SSQCOR, and GENVAR methods is of the same basic type, so they can be processed with one general computer program. When Torres et al. Torres et al. (2007) modelled the semantics of audio content, they used CCA to measure acoustic correlation to identify the words that are represented well. They imposed constraints on CCA that explicitly turned it into a vocabulary selection mechanism so that they could find words that are strongly characterized by audio representation from the semantic feature space and the acoustic feature space with high correlation. The CCA variant is called sparse CCA. Tenenhaus et al. ? presented a general framework for multiple and multiblock data analysis methods for the generalization of regularized canonical correlation analysis for three or more groups of variables,

namely the regularized generalized canonical correlation analysis (RGCCA) model, which combined the power of multiblock data analysis methods and the flexibility of partial least squares (PLS) path modelling. Since RGCCA has no analytical solution, a new monotone convergence algorithm based on the PLS model was proposed by Herman Wold to look for the fixed point of the stationary equation related to RGCCA. However, the quality and interpretability of components extracted by RGCCA may be affected by the activity and correlation of variables in each block. Determining which subsets of variables in each block important plays a key role in the relationship between blocks.

For this, Tenenhaus et al. extended RGCCA to sparse generalized canonical correlation analysis (SGCCA) in Tenenhaus et al. (2014), in which blocks are not necessarily completely connected. The objective function contains three schemes, g may be defined as $g(\mathbf{x}) = \mathbf{x}$ (Horst scheme), which is equivalent to the GCCA proposed by Horst in 1961 and 1965, and as $g(\mathbf{x}) = |\mathbf{x}|$ (centroid scheme) or $g(\mathbf{x}) = \mathbf{x}^2$ (factorial scheme), which are from the relevant literature of PLS Hanafi (2007). They provided a monotone iterative algorithm for SGCCA based on the RGCCA algorithm, in which they used the solution to the subproblem (LM-P1 for short) of maximizing a linear function on an ℓ_1 -norm ball and a unit ℓ_2 -norm sphere proposed in Witten et al. (2009) to calculate the external components. However, there is a little mistake in the solution to the subproblem (LM-P1) proposed in Witten et al. (2009), which may become the reason that the iterative algorithm for SGCCA is slow and not always convergent. For this, we are going to characterize the solution to the subproblem LM-P1, LM-P2 and LM-P3, which maximize a linear function on the intersection of an ℓ_1 -norm sphere and a unit ℓ_2 -norm sphere, an ℓ_1 -norm ball and a unit ℓ_2 -norm sphere, respectively. Then we will design more efficient block coordinate descent (BCD) algorithms for SGCCA and its two variants, called SGCCA-BCD1, SGCCA-BCD2 and SGCCA-BCD3, corresponding to the subproblems LM-P1, LM-P2 and LM-P3, respectively, prove that they all globally converge to their stationary points. We further propose gradient projected (GP) methods for SGCCA and its two variants when using the Horst scheme, called SGCCA-GP1, SGCCA-GP2 and SGCCA-GP3, corresponding to the subproblems LM-P1, LM-P2 and LM-P3, respectively, and prove that they all globally converge to their critical points.

This paper is organized as follows. Some notations and preliminaries are introduced, the original SGCCA model in Tenenhaus et al. (2014) and

their monotone iterative algorithm are reviewed in Section 2. Section 3 characterize the solutions to the subproblems LM-P1, LM-P2 and LM-P3. The improved BCD algorithms for SGCCA and its two variants are designed, and their convergence analysis are discussed in Section 4. The gradient projected (GP) methods for SGCCA and its two variants are proposed and their convergence analysis are built in Section 5. The experiments on artificial data and real glioma data are conducted to evaluate our proposed BCD algorithms and GP methods in Section 6. Finally, some conclusions are obtained.

2. Preliminaries

2.1. Notations

For convenience of the reader, we give the following notation. Let \mathbb{R}^n be the space of real n -vectors and \mathbb{R}_+^n be the nonnegative orthant of \mathbb{R}^n , i.e., $\mathbb{R}_+^n := \{\mathbf{x} \in \mathbb{R}^n : x_i \geq 0, i = 1, \dots, n\}$. On \mathbb{R}^n , the ℓ_2 (i.e., Euclidean) norm is indicated as $\|\cdot\|_2$ with the unit ℓ_2 ball (sphere) defined as $\mathbb{B}_2 := \{\mathbf{x} \in \mathbb{R}^n : \|\mathbf{x}\|_2 \leq 1\}$ ($\mathbb{S}_2 := \{\mathbf{x} \in \mathbb{R}^n : \|\mathbf{x}\|_2 = 1\}$), and the ℓ_1 norm is indicated as $\|\cdot\|_1$ with the ℓ_1 ball (sphere) with radius t denoted as $\mathbb{B}_1^t := \{\mathbf{x} \in \mathbb{R}^n : \|\mathbf{x}\|_1 \leq t\}$ ($\mathbb{S}_1^t := \{\mathbf{x} \in \mathbb{R}^n : \|\mathbf{x}\|_1 = t\}$). Without loss of the generality, it is assumed that $1 < t < \sqrt{n}$ in the later.

Let $\mathbf{1}$ denote the vector of all ones. Given $\mathbf{v} = (v_1, v_2, \dots, v_n)^T \in \mathbb{R}^n$, define \mathbf{v}^+ to be such that $v_i^+ = \max(v_i, 0)$ for $i = 1, \dots, n$, and $|\mathbf{v}| = (|v_1|, |v_2|, \dots, |v_n|)^T$. For $\lambda \geq 0$, the soft-thresholding operator S is defined by $S_\lambda(v) = \text{sign}(v) \max(0, |v| - \lambda)$, and

$$S_\lambda(\mathbf{v}) = (S_\lambda(v_1), S_\lambda(v_2), \dots, S_\lambda(v_n))^T = (|\mathbf{v}| - \lambda \mathbf{1})^+.$$

And let $C \subset \mathbb{R}^n$ be a nonempty closed set, the projection operator P_C onto C is defined by

$$P_C(\mathbf{v}) = \arg \min_{\mathbf{x} \in C} \|\mathbf{x} - \mathbf{v}\|_2^2.$$

Proposition 1. (*Proposition 2.1. in Liu et al. (2020)*) Let $\mathbf{x} = P_{\mathbb{B}_2 \cap \mathbb{B}_1^t}(\mathbf{v})$, $\mathbf{y} \in P_{\mathbb{S}_2 \cap \mathbb{B}_1^t}(\mathbf{v})$ and $\mathbf{z} \in P_{\mathbb{S}_2 \cap \mathbb{S}_1^t}(\mathbf{v})$, then $v_i x_i \geq 0$, $v_i y_i \geq 0$ and $v_i z_i \geq 0$ for $i = 1, \dots, n$.

Let $\Omega_1^t, \Omega_2^t, \Omega_3^t$ be the following constraint domain, $\Omega_1^t = \{\mathbf{y} \in \mathbb{R}^n : \|\mathbf{y}\|_1 \leq t, \|\mathbf{y}\|_2 \leq 1\} = \mathbb{B}_1^t \cap \mathbb{B}_2$, $\Omega_2^t = \{\mathbf{y} \in \mathbb{R}^n : \|\mathbf{y}\|_1 = t, \|\mathbf{y}\|_2 = 1\} = \mathbb{S}_1^t \cap \mathbb{S}_2$,

and $\Omega_3^t = \{\mathbf{y} \in \mathbb{R}^n : \|\mathbf{y}\|_1 \leq t, \|\mathbf{y}\|_2 = 1\} = \mathbb{B}_1^t \cap \mathbb{S}_2$. Then the projection subproblems onto $\mathbb{B}_1^t \cap \mathbb{B}_2$, $\mathbb{S}_1^t \cap \mathbb{S}_2$ and $\mathbb{B}_1^t \cap \mathbb{S}_2$ can be formulated into

$$P_{\Omega_1^t}(\mathbf{v}) = \arg \min_{\mathbf{x} \in \mathbb{R}^n} \|\mathbf{x} - \mathbf{v}\|_2^2, \quad \text{s.t.} \quad \|\mathbf{x}\|_1 \leq t, \quad \|\mathbf{x}\|_2 \leq 1, \quad (\text{P1})$$

$$P_{\Omega_2^t}(\mathbf{v}) = \arg \min_{\mathbf{x} \in \mathbb{R}^n} \|\mathbf{x} - \mathbf{v}\|_2^2, \quad \text{s.t.} \quad \|\mathbf{x}\|_1 = t, \quad \|\mathbf{x}\|_2 = 1, \quad (\text{P2})$$

$$P_{\Omega_3^t}(\mathbf{v}) = \arg \min_{\mathbf{x} \in \mathbb{R}^n} \|\mathbf{x} - \mathbf{v}\|_2^2, \quad \text{s.t.} \quad \|\mathbf{x}\|_1 \leq t, \quad \|\mathbf{x}\|_2 = 1, \quad (\text{P3})$$

respectively, where $\mathbf{v} \in \mathbb{R}^n$ is given.

Further, let $\Omega_1^{t+}, \Omega_2^{t+}, \Omega_3^{t+}$ be the corresponding part of $\Omega_1^t, \Omega_2^t, \Omega_3^t$ in the first quadrant, that is, $\Omega_1^{t+} = \{\mathbf{y} \in \mathbb{R}_+^n : \|\mathbf{y}\|_1 \leq t, \|\mathbf{y}\|_2 \leq 1\}$, $\Omega_2^{t+} = \{\mathbf{y} \in \mathbb{R}_+^n : \|\mathbf{y}\|_1 = t, \|\mathbf{y}\|_2 = 1\}$, and $\Omega_3^{t+} = \{\mathbf{y} \in \mathbb{R}_+^n : \|\mathbf{y}\|_1 \leq t, \|\mathbf{y}\|_2 = 1\}$. By Proposition 1, one can restrict the projection to the nonnegative case, that is, replacing \mathbf{v} by $|\mathbf{v}|$ and assigning the signs of the elements of \mathbf{v} to the solution afterward. Thus, one only needs to focus on the following projection problems restricted on \mathbb{R}_+^n corresponding to (P1), (P2) and (P3):

$$P_{\Omega_1^{t+}}(\mathbf{v}) = \arg \min_{\mathbf{x} \in \mathbb{R}_+^n} \|\mathbf{x} - \mathbf{v}\|_2^2, \quad \text{s.t.} \quad \|\mathbf{x}\|_1 \leq t, \quad \|\mathbf{x}\|_2 \leq 1, \quad (\text{P1}^+)$$

$$P_{\Omega_2^{t+}}(\mathbf{v}) = \arg \min_{\mathbf{x} \in \mathbb{R}_+^n} \|\mathbf{x} - \mathbf{v}\|_2^2, \quad \text{s.t.} \quad \|\mathbf{x}\|_1 = t, \quad \|\mathbf{x}\|_2 = 1, \quad (\text{P2}^+)$$

$$P_{\Omega_3^{t+}}(\mathbf{v}) = \arg \min_{\mathbf{x} \in \mathbb{R}_+^n} \|\mathbf{x} - \mathbf{v}\|_2^2, \quad \text{s.t.} \quad \|\mathbf{x}\|_1 \leq t, \quad \|\mathbf{x}\|_2 = 1, \quad (\text{P3}^+)$$

where $\mathbf{v} \in \mathbb{R}_+^n$ is a given vector.

2.2. The SGCCA model and its iterative algorithm

In this subsection, we review the SGCCA model proposed in Tenenhaus et al. (2014) and their iterative algorithm for SGCCA.

Let's take J variables out of n samples, denote the variable blocks as $\mathbf{X}_1, \mathbf{X}_2, \dots, \mathbf{X}_J \in \mathbb{R}^{n \times p_j}$, where p_j is the dimensionality of the given variable block. The connection relationship between blocks is regarded as a prior information and the design matrix $\mathbf{C} = \{c_{jk}\}$ is used to define the graph of connections, c_{jk} is equal to 1 if the blocks \mathbf{X}_j and \mathbf{X}_k are connected or 0 otherwise. In order to identify which variables of each block are active, the linear coefficient vector before the variable block should be limited to

be sparse. Then the SGCCA model can be expressed in the following form Tenenhaus et al. (2014):

$$\begin{aligned}
\arg \max_{\mathbf{a}_1, \mathbf{a}_2, \dots, \mathbf{a}_J} h(\mathbf{a}_1, \mathbf{a}_2, \dots, \mathbf{a}_J) &= \sum_{j,k=1; j \neq k}^J c_{jk} g(\text{cov}(\mathbf{X}_j \mathbf{a}_j, \mathbf{X}_k \mathbf{a}_k)) \\
&= \sum_{j,k=1; j \neq k}^J c_{jk} g\left(\frac{1}{n} \mathbf{a}_j^T \mathbf{X}_j^T \mathbf{X}_k \mathbf{a}_k\right) \quad (\text{SGCCA-P3}) \\
\text{s.t. } \quad &\|\mathbf{a}_j\|_2 = 1, \|\mathbf{a}_j\|_1 \leq s_j, j = 1, \dots, J
\end{aligned}$$

where $\text{cov}(\cdot, \cdot)$ stands for the covariance function, $g(x)$ is taken to be x (Horst scheme), $|x|$ (centroid scheme) or x^2 (factorial scheme), s_j is a positive constant that determines the amount of sparsity for \mathbf{a}_j , $j = 1, \dots, J$. The smaller s_j , the larger the degree of sparsity for \mathbf{a}_j . Note that the involved ℓ_1 constraint in the above model tends to enforce sparsity of the generalized canonical vector.

To obtain a monotonically convergent algorithm of the optimization problem (SGCCA-P3), Tenenhaus etc defined the inner components \mathbf{z}_j as follows Tenenhaus et al. (2014):

$$\mathbf{z}_j = \sum_{k=1, k \neq j} c_{jk} w(\text{cov}(\mathbf{X}_j \mathbf{a}_j, \mathbf{X}_k \mathbf{a}_k)) \mathbf{X}_k \mathbf{a}_k = \sum_{k=1, k \neq j} c_{jk} w\left(\frac{1}{n} \mathbf{a}_j^T \mathbf{X}_j^T \mathbf{X}_k \mathbf{a}_k\right) \mathbf{X}_k \mathbf{a}_k, \quad (2.1)$$

where $w(x) = (1/\phi)g'(x)$ with $\phi = 1$ for both the horst and centroid scheme, and $\phi = 2$ for the factorial scheme. By using the following equality (Proposition 1 in ?):

$$\sum_{j,k=1; j \neq k}^J c_{jk} g(\text{cov}(\mathbf{X}_j \mathbf{a}_j, \mathbf{X}_k \mathbf{a}_k)) = \sum_{j=1}^J \text{cov}(\mathbf{X}_j \mathbf{a}_j, \mathbf{z}_j), \quad (2.2)$$

Proposition 1 in Tenenhaus et al. (2014) proved the solution for the optimization problem (SGCCA-P3) satisfied

$$\mathbf{a}_j = \frac{S_{\lambda_{1j}}((1/n)\mathbf{X}_j^T \mathbf{z}_j)}{\|S_{\lambda_{1j}}((1/n)\mathbf{X}_j^T \mathbf{z}_j)\|_2}, \quad j = 1, \dots, J \quad (2.3)$$

where S is the soft-thresholding operator, and $\lambda_{2j}, \lambda_{1j}$ are chosen such that $\|\mathbf{a}_j\|_2 = 1$ and $\|\mathbf{a}_j\|_1 \leq s_j$.

Thus, Tenenhaus et al. (2014) gave the following iterative algorithm for SGCCA problem (SGCCA-P3) based on partial least square (PLS) method solving RGCCA in ?.

Algorithm 1 Sparse generalized canonical correlation analysis (SGCCA)

- 1: Input J blocks $\mathbf{X}_1, \dots, \mathbf{X}_J$, J ℓ_1 constraints s_1, \dots, s_J , a design matrix \mathbf{C} and the scheme, Choose J arbitrary normalized vectors $\mathbf{a}_1^0, \mathbf{a}_2^0, \dots, \mathbf{a}_J^0$.
 - 2: **repeat**
 - 3: ($s = 0, 1, 2, \dots$)
 - 4: **for** $j = 1, 2, \dots, J$ **do**
 - 5: Compute the inner components

$$\mathbf{z}_j^s \leftarrow \sum_{k=1}^{j-1} c_{jk} w(\text{cov}(\mathbf{X}_j \mathbf{a}_j^s, \mathbf{X}_k \mathbf{a}_k^{s+1})) \mathbf{X}_k \mathbf{a}_k^{s+1} + \sum_{k=j+1}^J c_{jk} w(\text{cov}(\mathbf{X}_j \mathbf{a}_j^s, \mathbf{X}_k \mathbf{a}_k^s)) \mathbf{X}_k \mathbf{a}_k^s$$
 - 6: Compute the outer weight

$$\mathbf{a}_j^{s+1} \leftarrow \frac{S_{\lambda_{1j}}(\frac{1}{n} \mathbf{X}_j^t \mathbf{z}_j^s)}{\|S_{\lambda_{1j}}(\frac{1}{n} \mathbf{X}_j^t \mathbf{z}_j^s)\|_2}$$

where S denotes the soft-thresholding operator and $\lambda_{1j} = 0$ if $\|\mathbf{a}_j^{s+1}\|_1 \leq s_j$ or λ_{1j} chosen such that $\|\mathbf{a}_j^s\|_1 = s_j$ (binary search) with $0 \leq s_j \leq \sqrt{p_j}$.
 - 7: **end for**
 - 8: **until** $h(\mathbf{a}_1^{s+1}, \dots, \mathbf{a}_J^{s+1}) - h(\mathbf{a}_1^s, \dots, \mathbf{a}_J^s) \leq \epsilon$
 - 9: Return $\mathbf{a}_1^{s+1}, \dots, \mathbf{a}_J^{s+1}$
-

In ?, Zhang etc proved the subproblems (P1) and (P3) are equivalent for the SCoTLASS model of sparse principal component analysis (SPCA) problem, and the solutions to the subproblems (P2) and (P3) are of little difference. We are curious that if the subproblems (P1) and (P3) are equivalent and the subproblems (P2) and (P3) are close for the SGCCA problem. So we provide the following two variants (SGCCA-P1) and (SGCCA-P2) of SGCCA problem:

$$\begin{aligned} \arg \max_{\mathbf{a}_1, \mathbf{a}_2, \dots, \mathbf{a}_J} \sum_{j,k=1; j \neq k}^J c_{jk} g(\text{cov}(\mathbf{X}_j \mathbf{a}_j, \mathbf{X}_k \mathbf{a}_k)) &= \sum_{j,k=1; j \neq k}^J c_{jk} g\left(\frac{1}{n} \mathbf{a}_j^T \mathbf{X}_j^T \mathbf{X}_k \mathbf{a}_k\right) \\ \text{s.t. } \|\mathbf{a}_j\|_2 &\leq 1, \|\mathbf{a}_j\|_1 \leq s_j, j = 1, \dots, J \end{aligned} \tag{SGCCA-P1}$$

$$\begin{aligned} \arg \max_{\mathbf{a}_1, \mathbf{a}_2, \dots, \mathbf{a}_J} \sum_{j,k=1; j \neq k}^J c_{jk} g(\text{cov}(\mathbf{X}_j \mathbf{a}_j, \mathbf{X}_k \mathbf{a}_k)) &= \sum_{j,k=1; j \neq k}^J c_{jk} g\left(\frac{1}{n} \mathbf{a}_j^T \mathbf{X}_j^T \mathbf{X}_k \mathbf{a}_k\right) \\ \text{s.t. } \|\mathbf{a}_j\|_2 &= 1, \|\mathbf{a}_j\|_1 = s_j, j = 1, \dots, J \end{aligned} \quad (\text{SGCCA-P2})$$

From (2.2), one easily knows that solving the SGCCA problem (SGCCA-P3), or its variant (SGCCA-P1) or (SGCCA-P2) is equivalent to solve the following problems (2.4), (2.5) or (2.6) for each $j = 1, \dots, J$, respectively:

$$\begin{aligned} \arg \max_{\mathbf{a}_j} \text{cov}(\mathbf{X}_j \mathbf{a}_j, \mathbf{z}_j) &= \arg \max_{\mathbf{a}_j} \langle \mathbf{X}_j^T \mathbf{z}_j, \mathbf{a}_j \rangle \\ \text{s.t. } \|\mathbf{a}_j\|_2 &= 1, \|\mathbf{a}_j\|_1 \leq s_j, \end{aligned} \quad (2.4)$$

$$\begin{aligned} \arg \max_{\mathbf{a}_j} \text{cov}(\mathbf{X}_j \mathbf{a}_j, \mathbf{z}_j) &= \arg \max_{\mathbf{a}_j} \langle \mathbf{X}_j^T \mathbf{z}_j, \mathbf{a}_j \rangle \\ \text{s.t. } \|\mathbf{a}_j\|_2 &\leq 1, \|\mathbf{a}_j\|_1 \leq s_j. \end{aligned} \quad (2.5)$$

$$\begin{aligned} \arg \max_{\mathbf{a}_j} \text{cov}(\mathbf{X}_j \mathbf{a}_j, \mathbf{z}_j) &= \arg \max_{\mathbf{a}_j} \langle \mathbf{X}_j^T \mathbf{z}_j, \mathbf{a}_j \rangle \\ \text{s.t. } \|\mathbf{a}_j\|_2 &= 1, \|\mathbf{a}_j\|_1 = s_j, \end{aligned} \quad (2.6)$$

where $\langle \cdot, \cdot \rangle$ is the notation of inner-product. Notice that for each $j = 1, \dots, J$, Tenenhaus etc in Tenenhaus et al. (2014) pointed out the solution (2.3) is also solution to the convex problem (2.5). We think the ‘‘convex’’ here meaning that one considers z_j as a constant relative to \mathbf{a}_j . But it is not correct for the centroid scheme $g(x) = |x|$ and the factorial scheme $g(x) = x^2$.

Remark 2. *The proof of Proposition 1 in Tenenhaus et al. (2014) is correct for the problem (SGCCA-P1) with $\lambda_{2j} > 0$ whenever using Horst, centroid or factorial scheme, and meanwhile, for each $j = 1, \dots, J$, the solution (2.3) is exactly the solution to the convex problem (2.5) when considering z_j as a constant relative to \mathbf{a}_j . And if $\lambda_{2j} > 0$ and $\lambda_{1j} \geq 0$ is taken to be such that $\|\mathbf{a}_j\|_2 = 1$, the solution (2.3) is also the solution to the problems (SGCCA-P3) and (2.4) when considering z_j as a constant relative to \mathbf{a}_j ; if $\lambda_{2j} > 0$ and $\lambda_{1j} \geq 0$ are taken to be such that $\|\mathbf{a}_j\|_2 = 1$ and $\|\mathbf{a}_j\|_1 = s_j$, the solution (2.3) is also the solution to the problems (SGCCA-P2) and (2.6) when considering z_j as a constant relative to \mathbf{a}_j . The case that $\lambda_{2j} = 0$ is corresponding to the case that (2.4), (2.5) and (2.6) have more solutions when considering z_j as a constant relative to \mathbf{a}_j , which we will characterize in next section.*

3. The linear function maximization problem on the intersection of an ℓ_1 -ball (sphere) and a unit ℓ_2 -ball (sphere)

When considering z_j as a constant relative to \mathbf{a}_j , the problems (2.4), (2.5) and (2.6) are essentially the linear function maximization problem on the intersection of an ℓ_1 -ball and a unit ℓ_2 -ball, an ℓ_1 -ball sphere and a unit ℓ_2 -sphere, and an ℓ_1 -ball and a unit ℓ_2 -sphere, respectively. For simplicity, we consider the constrained optimization problem on $\Omega_1^t = \mathbb{B}_1^t \cap \mathbb{B}_2$, $\Omega_2^t = \mathbb{S}_1^t \cap \mathbb{S}_2$ or $\Omega_3^t = \mathbb{B}_1^t \cap \mathbb{S}_2$, of general linear functions as follows:

$$\max_{\mathbf{x} \in \mathbb{R}^n} \langle \mathbf{v}, \mathbf{x} \rangle \quad \text{s.t.} \quad \|\mathbf{x}\|_2^2 \leq 1, \|\mathbf{x}\|_1 \leq t, \quad (\text{LM-P1})$$

$$\max_{\mathbf{x} \in \mathbb{R}^n} \langle \mathbf{v}, \mathbf{x} \rangle \quad \text{s.t.} \quad \|\mathbf{x}\|_2^2 = 1, \|\mathbf{x}\|_1 = t, \quad (\text{LM-P2})$$

$$\max_{\mathbf{x} \in \mathbb{R}^n} \langle \mathbf{v}, \mathbf{x} \rangle \quad \text{s.t.} \quad \|\mathbf{x}\|_2^2 = 1, \|\mathbf{x}\|_1 \leq t, \quad (\text{LM-P3})$$

where $\mathbf{v} \in \mathbb{R}^n$ is a given vector.

Witten et al. Witten et al. (2009) discussed the relation between problems (LM-P1) and (LM-P3) and point out provided that t is chosen appropriately, the solution to (LM-P1) satisfying $\|\mathbf{x}\|_2 = 1$ also solve (LM-P3). They characterizes the solution to (LM-P1) in the following lemma.

Lemma 3. (Witten et al. (2009), Lemma 2.2) *Consider the optimization problem (LM-P1), the solution satisfies $\mathbf{x} = \frac{S_\lambda(\mathbf{v})}{\|S_\lambda(\mathbf{v})\|_2}$, with $\lambda = 0$ if this results in $\|\mathbf{x}\|_1 \leq t$; otherwise, $\lambda > 0$ is chosen so that $\|\mathbf{x}\|_1 = t$, where S is the soft-thresholding operator.*

Remark 4. *A counterexample is that $n = 2$, $\mathbf{v} = (1, 1)$, $t = 1.2$. Obviously, any \mathbf{x} satisfying $x_1 + x_2 = 1.2$, $x_1^2 + x_2^2 \leq 1$, $x_1 \geq 0$, $x_2 \geq 0$ solves \mathbf{x} the problem (LM-P1) and (LM-P3). However, the solution given by Lemma 3 is $\mathbf{x} = (0.6, 0.6)^T$ with $\lambda = 0.4$.*

Therefore, the solution given in Witten et al. (2009) for (LM-P1) is imperfect. In addition, Zhao et al. proposed a BCD-SPCA method in Zhao et al. (2015), there they also portrayed the optimal solution to (LM-P3).

Lemma 5. (Zhao et al. (2015), Theorem 3) *Given $\mathbf{v} \in \mathbb{R}^n$, denote by (q_1, q_2, \dots, q_n) the permutation of $(1, 2, \dots, n)$ based on the ascending order*

of $|\mathbf{v}| = (|v_1|, |v_2|, \dots, |v_n|)^T$. And for $\lambda \geq 0$, let $f_\lambda(\mathbf{v}) = \frac{S_\lambda(\mathbf{v})}{\|S_\lambda(\mathbf{v})\|_2}$. Then the solution to (LM-P3) is given by

$$\mathbf{x}^*(\mathbf{v}) = \begin{cases} \emptyset, & t < 1 \\ f_{\lambda_k}(\mathbf{v}), & t \in [\|f_{|v_{q_k}|}(\mathbf{v})\|_1, \|f_{|v_{q_{k-1}}|}(\mathbf{v})\|_1) (k = 2, 3, \dots, n-1) \\ f_{\lambda_1}(\mathbf{v}), & t \in [\|f_{|v_{q_1}|}(\mathbf{v})\|_1, \sqrt{n}) \\ f_0(\mathbf{v}), & t \geq \sqrt{n} \end{cases} \quad (3.1)$$

where S is still the soft-threshold operator, for $k = 1, 2, \dots, n-1$,

$$\lambda_k = \frac{(m-t^2)(\sum_{i=1}^m a_i) - \sqrt{t^2(m-t^2)(m\sum_{i=1}^m a_i^2 - (\sum_{i=1}^m a_i)^2)}}{m(m-t^2)},$$

and $(a_1, a_2, \dots, a_m) = (|v_{q_k}|, |v_{q_{k+1}}|, \dots, |v_{q_n}|)$, $m = n - k + 1$.

Remark 6. Notice that the case $\|f_{|v_{q_k}|}(\mathbf{v})\|_1 = \|f_{|v_{q_{k-1}}|}(\mathbf{v})\|_1$ is possible to happen, which implies the interval $[\|f_{|v_{q_k}|}(\mathbf{v})\|_1, \|f_{|v_{q_{k-1}}|}(\mathbf{v})\|_1)$ may be an empty set, and the solution in (3.1) is not well defined. Whence the program will fall into an infinite loop and cannot be terminated. To this end, we aim at studying the structure of the solutions to the above three subproblems (LM-P1), (LM-P2) and (LM-P3). Notice that the constraint sets of the three problems are symmetric about the origin, similar to Proposition 1 one can get the following proposition.

Proposition 7. For any $\mathbf{v} \in \mathbb{R}^n$, suppose \mathbf{x} be the optimal solution for (LM-P1), (LM-P2) or (LM-P3). Then $v_i x_i \geq 0, i = 1, 2, \dots, n$.

Proof. Assume by contradiction that there exists i_0 such that $v_{i_0} x_{i_0} < 0$. Define $\hat{\mathbf{x}}$ such that $\hat{x}_{i_0} = -x_{i_0}$ and $\hat{x}_i = x_i$ for all $i \neq i_0$, implying $\|\hat{\mathbf{x}}\|_p = \|\mathbf{x}\|_p, p = 1, 2$. Therefore $\hat{\mathbf{x}}$ is feasible for (LM-P1) (LM-P2), (LM-P3). And

$$\hat{\mathbf{x}}^T \mathbf{v} - \mathbf{x}^T \mathbf{v} = (\hat{\mathbf{x}} - \mathbf{x})^T \mathbf{v} = -2v_{i_0} x_{i_0} > 0 \quad (3.2)$$

implying $\hat{\mathbf{x}}^T \mathbf{v} > \mathbf{x}^T \mathbf{v}$, which contradicts that \mathbf{x} is optimal solution. This completes the proof.

According to Proposition 7, it is enough to only consider non-negative case. That is, one can first replace \mathbf{v} with $|\mathbf{v}|$, solve the subproblems (LM-P1), (LM-P2) or (LM-P3) on the non-negative octant, then modify the signs

of the elements of the optimal solution \mathbf{x} according to the sign of \mathbf{v} . For this, consider the following subproblems (LM-P1⁺), (LM-P2⁺), and (LM-P3⁺):

$$\max_{\mathbf{x} \in \mathbb{R}_+^n} \langle \mathbf{v}, \mathbf{x} \rangle \quad \text{s.t.} \quad \|\mathbf{x}\|_2^2 \leq 1, \|\mathbf{x}\|_1 \leq t, \quad (\text{LM-P1}^+)$$

$$\max_{\mathbf{x} \in \mathbb{R}_+^n} \langle \mathbf{v}, \mathbf{x} \rangle \quad \text{s.t.} \quad \|\mathbf{x}\|_2^2 = 1, \|\mathbf{x}\|_1 = t, \quad (\text{LM-P2}^+)$$

$$\max_{\mathbf{x} \in \mathbb{R}_+^n} \langle \mathbf{v}, \mathbf{x} \rangle \quad \text{s.t.} \quad \|\mathbf{x}\|_2^2 = 1, \|\mathbf{x}\|_1 \leq t, \quad (\text{LM-P3}^+)$$

where $\mathbf{v} \in \mathbb{R}_+^n$ is given.

For the subproblems (LM-P2⁺) and (LM-P3⁺), we have the following results.

Proposition 8. (1) For $\mathbf{v} \in \mathbb{R}^n$, we have

$$\arg \max_{\mathbf{x} \in \Omega_2^t} \langle \mathbf{v}, \mathbf{x} \rangle = \arg \min_{\mathbf{x} \in \Omega_2^t} \frac{1}{2} \|\mathbf{v} - \mathbf{x}\|_2^2 = P_{\Omega_2^t}(\mathbf{v}),$$

$$\arg \max_{\mathbf{x} \in \Omega_3^t} \langle \mathbf{v}, \mathbf{x} \rangle = \arg \min_{\mathbf{x} \in \Omega_3^t} \frac{1}{2} \|\mathbf{v} - \mathbf{x}\|_2^2 = P_{\Omega_3^t}(\mathbf{v}),$$

(2) For $\mathbf{v} \in \mathbb{R}_+^n$,

$$\arg \max_{\mathbf{x} \in \Omega_2^{t+}} \langle \mathbf{v}, \mathbf{x} \rangle = \arg \min_{\mathbf{x} \in \Omega_2^{t+}} \frac{1}{2} \|\mathbf{v} - \mathbf{x}\|_2^2 = P_{\Omega_2^{t+}}(\mathbf{v}),$$

$$\arg \max_{\mathbf{x} \in \Omega_3^{t+}} \langle \mathbf{v}, \mathbf{x} \rangle = \arg \min_{\mathbf{x} \in \Omega_3^{t+}} \frac{1}{2} \|\mathbf{v} - \mathbf{x}\|_2^2 = P_{\Omega_3^{t+}}(\mathbf{v}),$$

Proof. We only prove the equalities in (1), and the proof is similar for the equalities in (2).

$$\begin{aligned} (1) \quad \arg \max_{\mathbf{x} \in \Omega_2^t} \langle \mathbf{v}, \mathbf{x} \rangle &= \arg \max_{\mathbf{x} \in \Omega_2^t} - \langle \mathbf{v}, \mathbf{x} \rangle \\ &= \arg \max_{\mathbf{x} \in \Omega_2^t} - \left\{ \frac{1}{2} \|\mathbf{x}\|_2^2 - \langle \mathbf{v}, \mathbf{x} \rangle + \frac{1}{2} \right\} \quad (\text{by } \|\mathbf{x}\|_2 = 1) \\ &= \arg \max_{\mathbf{x} \in \Omega_2^t} - \frac{1}{2} \|\mathbf{v} - \mathbf{x}\|_2^2 \\ &= \arg \min_{\mathbf{x} \in \Omega_2^t} \frac{1}{2} \|\mathbf{v} - \mathbf{x}\|_2^2 = P_{\Omega_2^t}(\mathbf{v}). \end{aligned}$$

The proof for Ω_3^t is similar.

From Proposition 8, it can be seen that the subproblems (LM-P2), (LM-P3), (LM-P2⁺) and (LM-P3⁺) are actually equivalent to the projection subproblems (P2), (P3), (P2⁺) and (P3⁺), respectively. Then one can solve the subproblems (LM-P2) and (LM-P3) using Algorithm 3 and Algorithm 4 in ?, respectively. Moreover, according to the solutions to (P2⁺) and (P3⁺) provided in Theorem 4.2 and Theorem 4.3 in Liu et al. (2020), respectively, and Remark 1 in ? (which provides a simple solution to the subproblems (P1⁺), (P2⁺) and (P3⁺) for the case that the solution is not unique), we can get a solution to (LM-P2⁺) and a solution to (LM-P3⁺) as follows.

Let $\mathbf{v} \in \mathbb{R}^n$, v_{\max} denote the largest component of \mathbf{v} . For simplicity, it is assumed that $\lambda_j, j = 1, \dots, k$ are the k distinct components of \mathbf{v} such that $\lambda_1 > \dots > \lambda_k$ with $\lambda_1 = v_{\max}$. $\mathcal{I}_j = \{i : v_i \geq \lambda_j, i = 1, \dots, n\}$, $I_j = |\mathcal{I}_j|$. Let \mathbf{e}_i be the canonical unit vector with the i th component 1; and $\mathbf{e}_{\mathcal{I}_1}$ denote the vector with the i th component 1 for $i \in \mathcal{I}_1$, and 0 for others.

Theorem 9. For $\mathbf{v} \in \mathbb{R}_+^n$, the optimal solution of (LM-P2⁺) can be given by

$$\mathbf{x}^* = \begin{cases} \frac{(\mathbf{v} - \lambda^* \mathbf{1})^+}{\|(\mathbf{v} - \lambda^* \mathbf{1})^+\|_2}, & I_1 < t^2, \\ \frac{1}{\sqrt{I_1}} \mathbf{e}_{\mathcal{I}_1}, & I_1 = t^2, \\ \alpha \mathbf{e}_{\mathcal{I}_1} + \beta \mathbf{e}_1, & I_1 > t^2. \end{cases} \quad (3.3)$$

where $\alpha = \frac{1}{I_1} (t - \sqrt{\frac{I_1 - t^2}{I_1 - 1}})$, $\beta = \sqrt{\frac{I_1 - t^2}{I_1 - 1}}$.

Theorem 10. For $\mathbf{v} \in \mathbb{R}_+^n$, the optimal solution of (LM-P3⁺) can be given by

$$\mathbf{x}^* = \begin{cases} \frac{(\mathbf{v} - \lambda^* \mathbf{1})^+}{\|(\mathbf{v} - \lambda^* \mathbf{1})^+\|_2}, & I_1 \leq t^2, \|\mathbf{v}\|_1 > t\|\mathbf{v}\|_2, \\ \frac{\mathbf{v}}{\|\mathbf{v}\|_2}, & I_1 \leq t^2, \|\mathbf{v}\|_1 \leq t\|\mathbf{v}\|_2, \\ \alpha \mathbf{e}_{\mathcal{I}_1} + \beta \mathbf{e}_1, & I_1 > t^2. \end{cases} \quad (3.4)$$

where $\alpha = \frac{1}{I_1} (t - \sqrt{\frac{I_1 - t^2}{I_1 - 1}})$, $\beta = \sqrt{\frac{I_1 - t^2}{I_1 - 1}}$.

Remark 11. From Proposition 8, Theorem 9, Theorem 10 and Remark 2 in ? we know the solutions to (LM-P2⁺) and (LM-P3⁺) are the same except the case of $I_1 < t^2$ and $\|\mathbf{v}\|_1 \leq t\|\mathbf{v}\|_2$.

Then we investigate the subproblem (LM-P1⁺). It is easy to see that (LM-P1⁺) is convex. We now get its solution with the help of the Lagrangian duality theory. The dual objective is given by

$$g(\lambda, \mu) = \inf_{\mathbf{x} \in \mathbb{R}_+^n} L(\mathbf{x}, \lambda, \mu) := -\langle \mathbf{v}, \mathbf{x} \rangle + \lambda(\|\mathbf{x}\|_1 - t) + \frac{\mu}{2}(\|\mathbf{x}\|_2^2 - 1), \quad (3.5)$$

where $L(\mathbf{x}, \lambda, \mu)$ is the partial Lagrangian with the dual variables $\lambda \geq 0, \mu \geq 0$. The properties of g are analyzed in the following lemma.

Lemma 12. For given $\lambda, \mu \in \mathbb{R}$, the followings hold.

(i) Suppose $\mu = 0$. If $\lambda > v_{\max}$, then the solution of (3.5) is $\mathbf{x} = 0$, and $g(\lambda, \mu) = -\lambda t$. If $\lambda = v_{\max}$, then the solution of (3.5) is any \mathbf{x} satisfying

$$x_i \geq 0, i \in \mathcal{I}_1; x_i = 0, i \notin \mathcal{I}_1, \quad (3.6)$$

meanwhile, $g(\lambda, \mu) = -\lambda t$. If $\lambda < v_{\max}$, then $g(\lambda, \mu) = -\infty$.

(ii) Suppose $\mu > 0$. The solution of (3.5) is

$$\mathbf{x}(\lambda, \mu) = \frac{(\mathbf{v} - \lambda \mathbf{1})^+}{\mu} \quad (3.7)$$

with dual objective being

$$g(\lambda, \mu) = -\lambda t - \frac{\mu}{2} - \frac{1}{2\mu} \|(\mathbf{v} - \lambda \mathbf{1})^+\|_2^2 \quad (3.8)$$

and the gradient

$$\begin{aligned} \frac{\partial g}{\partial \lambda} &= \frac{1}{\mu} \|(\mathbf{v} - \lambda \mathbf{1})^+\|_1 - t \\ \frac{\partial g}{\partial \mu} &= \frac{1}{2\mu^2} \|(\mathbf{v} - \lambda \mathbf{1})^+\|_2^2 - \frac{1}{2} \end{aligned} \quad (3.9)$$

Moreover, (λ^*, μ^*) is a stationary point for $g(\lambda, \mu)$ if and only if $\phi(\lambda^*) = 0$ with $\lambda^* \in (-\infty, v_{\max})$ and $\mu^* = \|(\mathbf{v} - \lambda^* \mathbf{1})^+\|_2$, where $\phi(\lambda) = \|(\mathbf{v} - \lambda \mathbf{1})^+\|_1^2 - t^2 \|(\mathbf{v} - \lambda \mathbf{1})^+\|_2^2$ defined in Liu et al. (2020). In addition, $\mathbf{x}(\lambda^*, \mu^*) = \frac{(\mathbf{v} - \lambda^* \mathbf{1})^+}{\|(\mathbf{v} - \lambda^* \mathbf{1})^+\|_2}$.

Proof. (i) Suppose $\mu = 0$, We have $L(\mathbf{x}, \lambda, \mu) = (\lambda \mathbf{1} - \mathbf{v})^T \mathbf{x} - \lambda t$. We can see (i) holds trivially.

(ii) Suppose $\mu > 0$. Let $\boldsymbol{\zeta} \in \mathbb{R}_+^n$ be the multiplier for $\mathbf{x} \geq 0$, from KKT conditions the optimal $(\mathbf{x}, \lambda, \mu, \boldsymbol{\zeta})$ for (LM-P1⁺) must satisfy

$$-\mathbf{v} + \lambda \mathbf{1} + \mu \mathbf{x} - \boldsymbol{\zeta} = 0, \quad \mathbf{x} \geq 0, \quad \boldsymbol{\zeta} \geq 0, \quad x_i \zeta_i = 0, \quad i = 1, \dots, n \quad (3.10)$$

Then we have if $x_i > 0$, meaning $\zeta_i = 0$, it easily follows that $x_i = \frac{1}{\mu}(v_i - \lambda)$; if $x_i = 0$, it follows that $v_i - \lambda = -\zeta_i \leq 0$. Therefore, $\mathbf{x}(\lambda, \mu) = \frac{(\mathbf{v} - \lambda \mathbf{1})^+}{\mu}$, that is, (3.7) is true. Meanwhile, we have the dual objective

$$\begin{aligned} g(\lambda, \mu) &= -\langle \mathbf{v}, \mathbf{x} \rangle + \lambda(\|\mathbf{x}\|_1 - t) + \frac{\mu}{2}(\|\mathbf{x}\|_2^2 - 1) \\ &= -\lambda t - \frac{\mu}{2} + (\lambda \mathbf{1} - \mathbf{v})^T \frac{1}{\mu}(\mathbf{v} - \lambda \mathbf{1})^+ + \frac{\mu}{2} \frac{1}{\mu^2} \|(\mathbf{v} - \lambda \mathbf{1})^+\|_2^2 \\ &= -\lambda t - \frac{\mu}{2} - \frac{1}{2\mu} \|(\mathbf{v} - \lambda \mathbf{1})^+\|_2^2, \end{aligned}$$

and

$$\begin{aligned} \frac{\partial g}{\partial \lambda} &= -t - \frac{1}{\mu}(-\mathbf{1})^T(\mathbf{v} - \lambda \mathbf{1})^+ = \frac{1}{\mu} \|(\mathbf{v} - \lambda \mathbf{1})^+\|_1 - t, \\ \frac{\partial g}{\partial \mu} &= -\frac{1}{2} - \frac{1}{2} \|(\mathbf{v} - \lambda \mathbf{1})^+\|_2^2 \cdot \left(-\frac{1}{\mu^2}\right) = \frac{1}{2\mu^2} \|(\mathbf{v} - \lambda \mathbf{1})^+\|_2^2 - \frac{1}{2}, \end{aligned}$$

that is, (3.8) and (3.9) hold. Now suppose that (λ^*, μ^*) is stationary for g . It holds that $\nabla g(\lambda^*, \mu^*) = 0$, implying $\lambda^* \in (-\infty, v_{\max})$ (otherwise, $\frac{\partial g}{\partial \lambda^*} = -t \neq 0$). Using (3.9) we have $\mu^* = \frac{\|(\mathbf{v} - \lambda^* \mathbf{1})^+\|_1}{t}$, and $\mu^* = \|(\mathbf{v} - \lambda^* \mathbf{1})^+\|_2$, therefore,

$$\phi(\lambda^*) = \|(\mathbf{v} - \lambda^* \mathbf{1})^+\|_1^2 - t^2 \|(\mathbf{v} - \lambda^* \mathbf{1})^+\|_2^2 = t^2 \mu^{*2} - t^2 \mu^{*2} = 0.$$

Conversely, if $\phi(\lambda^*) = 0$ with $\lambda^* \in (-\infty, v_{\max})$, letting $\mu^* = \|(\mathbf{v} - \lambda^* \mathbf{1})^+\|_2$. Substitute this expression into the formulas in (3.9), it easily follows that $\nabla g(\lambda^*, \mu^*) = 0$, hence (λ^*, μ^*) is stationary for g , and from (3.7) we get $\mathbf{x}^* = \mathbf{x}(\lambda^*, \mu^*) = \frac{(\mathbf{v} - \lambda^* \mathbf{1})^+}{\|(\mathbf{v} - \lambda^* \mathbf{1})^+\|_2}$. This completes the proof of part (ii). \square

Now it remains to solve dual problem

$$\begin{aligned} \max \quad & g(\lambda, \mu) \\ \text{s.t.} \quad & \lambda \geq 0, \mu \geq 0 \end{aligned} \tag{3.11}$$

Notice that the subproblem (LM-P1⁺) is a convex and satisfies the Slater condition. Let (λ^*, μ^*) solve dual problem (3.11), according to the KKT conditions, if for a given (λ^*, μ^*) , the solution of the problem (LM-P1⁺) is feasible, and satisfies the complementary relaxation condition $\lambda^*(\mathbf{1}^T \mathbf{x}^* - t) = 0$ and $\mu^*(\|\mathbf{x}^*\|_2^2 - 1) = 0$, then $\mathbf{x}^* = \mathbf{x}(\lambda^*, \mu^*)$ is the optimal solution of (LM-P1⁺). In the following, by characterizing the optimal solution of the dual problem (3.11), the optimal solution of the original problem (LM-P1⁺) can be obtained.

Theorem 13. *For any $\mathbf{v} \in \mathbb{R}_+^n$, the following statements must be true:*

(i) *If $I_1 \leq t^2$, then (LM-P1⁺) has a unique solution \mathbf{x}^* . If $\|\mathbf{v}\|_1 > t\|\mathbf{v}\|_2$, $\mathbf{x}^* = \frac{(\mathbf{v} - \lambda^* \mathbf{1})^+}{\|(\mathbf{v} - \lambda^* \mathbf{1})^+\|_2}$ with λ^* the unique root of the equation $\phi(\lambda) = 0$ in $(0, v_{\max})$, where $\phi(\lambda) = \|(\mathbf{v} - \lambda \mathbf{1})^+\|_1^2 - t^2 \|(\mathbf{v} - \lambda \mathbf{1})^+\|_2^2$ defined in Liu et al. (2020).*

(ii) *If $I_1 \leq t^2$ and $\|\mathbf{v}\|_1 \leq t\|\mathbf{v}\|_2$, (LM-P1⁺) has a unique solution $\mathbf{x}^* = \frac{\mathbf{v}}{\|\mathbf{v}\|_2}$.*

(iii) *If $I_1 > t^2$, the solution of (LM-P1⁺) is not unique. Its solutions are same with that of the system*

$$\sum_{i \in \mathcal{I}_1} x_i = t, \sum_{i \in \mathcal{I}_1} x_i^2 \leq 1, x_i \geq 0, i \in \mathcal{I}_1, x_i = 0, i \notin \mathcal{I}_1 \tag{3.12}$$

(iv) *If $v_{\max} = 0$, the feasible solutions of (LM-P1⁺) are all optimal.*

Proof. (i) If $I_1 = t^2$, by Corollary 3.1(i) in Liu et al. (2020), for any $\lambda \in [\lambda_2, v_{\max})$, $\phi(\lambda) = 0$; If $I_1 < t^2$, notice that $\|\mathbf{v}\|_1 > t\|\mathbf{v}\|_2$ is equivalent to $\phi(0) > 0$, we know from Corollary 3.1(ii) in Liu et al. (2020), $\phi(\lambda) = 0$ has a unique root λ^* in the interval $(0, v_{\max})$. In both cases, set $\mu^* = \|(\mathbf{v} - \lambda^* \mathbf{1})^+\|_2 > 0$. From Lemma 12(ii) we know that (λ^*, μ^*) is the stationary point of the dual objective $g(\lambda, \mu)$, that is, $\nabla g(\lambda^*, \mu^*) = 0$, and $\mathbf{x}^* = \mathbf{x}(\lambda^*, \mu^*) = \frac{(\mathbf{v} - \lambda^* \mathbf{1})^+}{\|(\mathbf{v} - \lambda^* \mathbf{1})^+\|_2}$ is the only optimal solution to the dual function (3.5) (when $I_1 = t^2$, the unique solution is just the vector with the

i th component $\frac{1}{I_1}$ for $i \in \mathcal{I}_1$, and 0 for others), and also a feasible solution to the problem (LM-P1⁺). Thus $\mathbf{x}^* = \mathbf{x}(\lambda^*, \mu^*)$ is the optimal solution of (LM-P1⁺). Case (i) is proved.

(ii) If $I_1 \leq t^2$ and $\|\mathbf{v}\|_1 \leq t\|\mathbf{v}\|_2$, the same argument as for case (i) implies that $\mu^* = \|(\mathbf{v} - \lambda^*\mathbf{1})^+\|_2 > 0$. Since $\|\mathbf{v}\|_1 \leq t\|\mathbf{v}\|_2$, letting (λ^*, μ^*) with $\lambda^* = 0, \mu^* = \|\mathbf{v}\|_2$, according to the first-order optimality condition of solving the duality problem (3.11), for any $\lambda \geq 0, \mu \geq 0$,

$$\begin{aligned} & \frac{\partial g(\lambda^*, \mu^*)}{\partial \lambda}(\lambda - \lambda^*) + \frac{\partial g(\lambda^*, \mu^*)}{\partial \mu}(\mu - \mu^*) \\ &= \left(\frac{\|\mathbf{v}\|_1}{\|\mathbf{v}\|_2} - t \right) \lambda + 0(\mu - \mu^*) \leq 0 \end{aligned}$$

Therefore, (λ^*, μ^*) is optimal for (3.11). Correspondingly $\mathbf{x}^* = \mathbf{x}(\lambda^*, \mu^*) = \frac{\mathbf{v}}{\|\mathbf{v}\|_2}$, which is also feasible for (LM-P1⁺). Therefore, $\mathbf{x}^* = \mathbf{x}(\lambda^*, \mu^*)$ is optimal for (LM-P1⁺). Case (ii) is proved.

(iii) Suppose $I_1 > t^2$. By the Corollary 3.1(i) in Liu et al. (2020), $\phi(\lambda) = 0$ has no root in $(-\infty, v_{\max})$. According to Lemma 12(ii), $g(\lambda, \mu)$ has no stationary point in the region $\mathbb{R} \times (0, \infty)$, which implies $\mu^* = 0$. And from Lemma 12(i), the optimal solution of dual problem (3.11) must be $(\lambda^*, \mu^*) = (v_{\max}, 0)$. Meanwhile, any \mathbf{x} satisfying (3.12) must be a solution of dual problem (3.11) since it meets (3.6). Moreover, it also meets the constraints of (LM-P1⁺). And it is easily verified that any \mathbf{x} satisfying (3.12) with $\lambda^* = v_{\max}$ and $\mu^* = 0$ meets the complementarity condition $\lambda^*(\|\mathbf{x}\|_1 - t) = 0$ and $\mu^*(\|\mathbf{x}\|_2^2 - 1) = 0$. Thus, any \mathbf{x} satisfying (3.12) is also optimal for problem (LM-P1⁺), Case (iii) is proved.

(iv) If $v_{\max} = 0$, we see $\mathbf{v} = \mathbf{0}$, the objective function is a constant function, and all feasible solutions are optimal. This completes the proof. \square

According to Theorem 13 and Remark 1 in ?, we can obtain the following analytic solution to the subproblem (LM-P1⁺).

Theorem 14. For $\mathbf{v} \in \mathbb{R}_+^n$, the optimal solution of (LM-P1⁺) can be given by

$$\mathbf{x}^* = \begin{cases} \frac{(\mathbf{v} - \lambda^*\mathbf{1})^+}{\|(\mathbf{v} - \lambda^*\mathbf{1})^+\|_2}, & I_1 \leq t^2, \|\mathbf{v}\|_1 > t\|\mathbf{v}\|_2, \\ \frac{\mathbf{v}}{\|\mathbf{v}\|_2}, & I_1 \leq t^2, \|\mathbf{v}\|_1 \leq t\|\mathbf{v}\|_2, \\ \alpha \mathbf{e}_{\mathcal{I}_1} + \beta \mathbf{e}_1, & I_1 > t^2, \end{cases} \quad (3.13)$$

where $\alpha = \frac{1}{I_1}(t - \sqrt{\frac{I_1 - t^2}{I_1 - 1}})$, $\beta = \sqrt{\frac{I_1 - t^2}{I_1 - 1}}$.

Remark 15. (1) From Theorem 10 and Theorem 14 we can see that the solutions to (LM-P1⁺) and (LM-P3⁺) are the same, and consequently the solutions to (LM-P1) and (LM-P3) are also the same. In fact, the assertion can be obtained by the proof of Theorem 6 in ?, there the authors proved that the set of extreme points of Ω_1^t is exactly Ω_3^t . Since Ω_1^t is a convex set and linear functions are concave, then by Corollary 32.3.2 in ?, the maximum of $\langle \mathbf{v}, \mathbf{x} \rangle$ on Ω_1^t exists and is obtained at some extreme point of Ω_1^t , that is, at some point of Ω_3^t .

(2) The solution of (LM-P1), (LM-P2) or (LM-P3) is $\tilde{\mathbf{x}}^* = \text{sign}(\mathbf{v}) \odot \mathbf{x}^*$, where \mathbf{x}^* is the solution of (LM-P1⁺), (LM-P2⁺) or (LM-P3⁺), and \odot is the Hadamard product.

4. The improved iterative algorithm for SGCCA problem and its variants

4.1. Block coordinate descent algorithms for SGCCA problem and its variants based on linear function maximization

From the explanation in Remark 2 we know that the problems (2.4), (2.5) and (2.6) can be seen as linear function maximization (LFM) problems (LM-P3), (LM-P1) and (LM-P2), respectively, by viewing the inner components z_j as constants. Meanwhile, the objective function of the problems (2.4) is a sum of linear functions about \mathbf{a}_j , and the constraint set is separable for every coefficient variable, and then the original iterative algorithm for SGCCA in Tenenhaus et al. (2014) is actually a block coordinate descent (BCD) algorithm. If, instead, we use the formulas of the optimal solution to LFM in Theorem 9, Theorem 10 and Theorem 14 to compute the outer weight, then the improved BCD algorithm for SGCCA problem and its variants can be designed as in Algorithm 2.

Remark 16. We use the QASB method proposed in Liu et al. (2020) to calculate the root of $\phi(\lambda) = 0$ in the process of the outer weight computation in Algorithm 2.

Algorithm 2 Block coordinate descent algorithm for SGCCA problem and its variants based on linear function maximization (SGCCA-BCD1, SGCCA-BCD2 or SGCCA-BCD3 corresponding to projection subproblems (P1),(P2) or (P3), respectively)

- 1: Input J blocks $\mathbf{X}_1, \dots, \mathbf{X}_J$, J ℓ_1 constraints s_1, \dots, s_J , a design matrix \mathbf{C} and the scheme, choose J arbitrary normalized vectors $\mathbf{a}_1^0, \mathbf{a}_2^0, \dots, \mathbf{a}_J^0$.
 - 2: **repeat**
 - 3: ($s = 0, 1, 2, \dots$)
 - 4: **for** $j = 1, 2, \dots, J$ **do**
 - 5: Compute the inner components

$$\mathbf{z}_j^s \leftarrow \sum_{k=1}^{j-1} c_{jk} w(\text{cov}(\mathbf{X}_j \mathbf{a}_j^s, \mathbf{X}_k \mathbf{a}_k^{s+1})) \mathbf{X}_k \mathbf{a}_k^{s+1} + \sum_{k=j+1}^J c_{jk} w(\text{cov}(\mathbf{X}_j \mathbf{a}_j^s, \mathbf{X}_k \mathbf{a}_k^s)) \mathbf{X}_k \mathbf{a}_k^s$$
 - 6: Compute the outer weight
calculate the coefficient vector \mathbf{a}_j^{s+1} according to the formula (3.3), (3.4) or (3.13), respectively, where \mathbf{v} is taken to be $\mathbf{X}_j^T \mathbf{z}_j^s$.
 - 7: **end for**
 - 8: **until** $h(\mathbf{a}_1^{s+1}, \dots, \mathbf{a}_J^{s+1}) - h(\mathbf{a}_1^s, \dots, \mathbf{a}_J^s) \leq \epsilon$
 - 9: Return $\mathbf{a}_1^{s+1}, \dots, \mathbf{a}_J^{s+1}$
-

4.2. Convergence analysis for the proposed BCD algorithm

It has been proved in Tenenhaus et al. (2014) that objective function value sequence of the original SGCCA algorithm is monotone increasing as follows:

$$\forall s, h(\mathbf{a}_1^s, \dots, \mathbf{a}_J^s) \leq h(\mathbf{a}_1^{s+1}, \dots, \mathbf{a}_J^{s+1}) \quad (4.1)$$

In fact, since the original iterative algorithm is a BCD algorithm, other variables are fixed when the variable \mathbf{a}_j is updated every time, the monotone increasing of objective can be guaranteed by the proof of Theorem 4.1 in Tseng (2001).

Next, we analyze the convergence of the proposed BCD algorithms based on linear function maximization. Firstly, we construct the following function for the SGCCA problem and its variants.

$$f(\mathbf{a}_1, \mathbf{a}_2, \dots, \mathbf{a}_J) = -h(\mathbf{a}_1, \mathbf{a}_2, \dots, \mathbf{a}_J) + \sum_{j=1}^J f_j(\mathbf{a}_j) \quad (4.2)$$

where

$$h(\mathbf{a}_1, \mathbf{a}_2, \dots, \mathbf{a}_J) = \sum_{j=1}^J \text{cov}(\mathbf{X}_j \mathbf{a}_j, \mathbf{z}_j) = \frac{1}{n} \sum_{j=1}^J \langle \mathbf{X}_j^T \mathbf{z}_j, \mathbf{a}_j \rangle,$$

and for any $j = 1, \dots, J$, $f_j(\mathbf{a}_j)$ is the indicator function defined by

$$f_j(\mathbf{a}_j) = \begin{cases} 0, & \text{if } \mathbf{a}_j \in \Omega_1^{s_j}, \Omega_2^{s_j} \text{ or } \Omega_3^{s_j} \\ \infty, & \text{otherwise} \end{cases} \quad (4.3)$$

It can be seen that the constrained optimization problem SGCCA is equivalent to the following unconstrained optimization problem

$$\min_{\mathbf{a}_1, \mathbf{a}_2, \dots, \mathbf{a}_J} f(\mathbf{a}_1, \mathbf{a}_2, \dots, \mathbf{a}_J) \quad (4.4)$$

Using BCD algorithm to solve alternately $\mathbf{a}_j, j = 1, 2, \dots, J$. The following theorem holds.

Theorem 17. (*Convergence of the proposed BCD algorithm*) *The sequence $(\mathbf{a}_1, \mathbf{a}_2, \dots, \mathbf{a}_J)$ generated by the proposed algorithms SGCCA-BCD1, SGCCA-BCD2 and SGCCA-BCD3 converges to their stationary points.*

Proof. According to Theorem 4.1(c) in Tseng (2001), if $f(\mathbf{a}_1, \dots, \mathbf{a}_J)$ has at most one minimum in \mathbf{a}_j for $j = 1, \dots, J$, then every cluster point \mathbf{z} of \mathbf{a}_j is a coordinatewise minimum point of f . In addition, if f is regular at \mathbf{z} , then \mathbf{z} is a stationary point of f .

By the definition of the objective function f , we see $\text{dom}(h)$ is an open set, and h is Gâteaux-differentiable on $\text{dom}(h)$, based on Lemma 3.1 in Tseng (2001), h is regular on $\text{dom}f_0$. And according to formulas (3.3), (3.4), (3.13), we easily see that $f(\mathbf{a}_1, \dots, \mathbf{a}_J)$ has a unique minimum in each \mathbf{a}_j with others fixed. The above theorem then naturally follows from Theorem 4.1(c) in Tseng (2001).

5. The gradient projected method for SGCCA problem and its variants when using Horst scheme

From Theorem 4.1, Theorem 4.2 and Theorem 4.3 in Liu et al. (2020), we know the projection subproblems (LM-P1), (LM-P2) and (LM-P3) can be easily computed. So we can also design a gradient projected (GP) algorithm for SGCCA problem and its variants. As the gradient of the objective function is also easily computed when using Horst scheme, we only consider the case of $g(\mathbf{x}) = \mathbf{x}$ in this section.

5.1. The design of the gradient projected algorithm for SGCCA and its variants

Firstly we compute the gradient of the objective function

$$h(\mathbf{a}) = h(\mathbf{a}_1, \mathbf{a}_2, \dots, \mathbf{a}_J) = \sum_{j,k=1;j \neq k}^J c_{jk} g(\text{COV}(\mathbf{X}_j \mathbf{a}_j, \mathbf{X}_k \mathbf{a}_k)) = \frac{1}{n} \sum_{j,k=1;j \neq k}^J c_{jk} \mathbf{a}_j^T \mathbf{X}_j^T \mathbf{X}_k \mathbf{a}_k.$$

It easily follows that

$$\nabla h(\mathbf{a}) = \nabla h(\mathbf{a}_1, \mathbf{a}_2, \dots, \mathbf{a}_J) = [\nabla h(\mathbf{a}_1)^T, \nabla h(\mathbf{a}_2)^T, \dots, \nabla h(\mathbf{a}_J)^T]^T \quad (5.1)$$

where for $l = 1, \dots, J$,

$$\nabla h(\mathbf{a}_l) = \frac{1}{n} \sum_{j=1, j \neq l}^J c_{jl} (\mathbf{a}_j^T \mathbf{X}_j^T \mathbf{X}_l)^T + \frac{1}{n} \sum_{k=1, k \neq l}^J c_{lk} (\mathbf{X}_l^T \mathbf{X}_k \mathbf{a}_k) = \frac{2}{n} \sum_{k=1, k \neq l}^J c_{lk} (\mathbf{X}_l^T \mathbf{X}_k \mathbf{a}_k).$$

Then the gradient step of the GP algorithm for each iteration will be

$$\mathbf{a}^s + r_s \nabla h(\mathbf{a}^s) = \begin{pmatrix} \mathbf{a}_1^s \\ \mathbf{a}_2^s \\ \vdots \\ \mathbf{a}_J^s \end{pmatrix} + r_s \begin{pmatrix} \nabla h(\mathbf{a}_1)^T \\ \nabla h(\mathbf{a}_2)^T \\ \vdots \\ \nabla h(\mathbf{a}_J)^T \end{pmatrix} \quad (5.2)$$

where r_s is the step size.

Secondly, the projection step will be carried on. Denote by $\Omega_i = \Omega_i^{s_1} \times \Omega_i^{s_2} \times \dots \times \Omega_i^{s_J}$, $i = 1, 2, 3$, we need to compute the projection $P_{\Omega_i}(\mathbf{a}^s + \gamma_s \nabla h(\mathbf{a}^s))$, $i=1, 2$, or 3 . Since for $i = 1, 2, 3$, each $\Omega_i^{s_j}$, $j = 1, 2, \dots, J$ is a closed set in \mathbb{R}^{p_j} , it easily follows that Ω_i , $i = 1, 2, 3$ are all closed sets in $\mathbb{R}^{p_1} \times \mathbb{R}^{p_2} \times \dots \times \mathbb{R}^{p_J}$. And notice that for each vector block \mathbf{a}_i , the projection operation is separable. In fact, we have the following proposition.

Proposition 18. *Let $\mathbf{b} = (\mathbf{b}_1, \mathbf{b}_2, \dots, \mathbf{b}_J)^T$, $\mathbf{a}^* = (\mathbf{a}_1^*, \mathbf{a}_2^*, \dots, \mathbf{a}_J^*)^T \in \mathbb{R}^{p_1} \times \mathbb{R}^{p_2} \times \dots \times \mathbb{R}^{p_J}$, $i = 1, 2, 3$. Then $\mathbf{a}^* = P_{\Omega_i}(\mathbf{b})$ if and only if $\mathbf{a}_j^* = P_{\Omega_i^{s_j}}(\mathbf{b}_j)$, $\forall j = 1, 2, \dots, J$. In other words, $\mathbf{a}^* = \arg \min_{\mathbf{a} \in \Omega_i} \|\mathbf{b} - \mathbf{a}\|_2^2$ is equivalent to $\mathbf{a}_j^* = \arg \min_{\mathbf{a}_j \in \Omega_i^{s_j}} \|\mathbf{b}_j - \mathbf{a}_j\|_2^2$, $j = 1, 2, \dots, J$.*

Proof. Suppose that $\mathbf{a}_j^* = \arg \min_{\mathbf{a}_j \in \Omega_i^{s_j}} \|\mathbf{b}_j - \mathbf{a}_j\|_2^2, j = 1, \dots, J$. We know that $\mathbf{a}_j^* \in \Omega_i^{s_j}$ for $\Omega_i^{s_j}, j = 1, 2, \dots, J$ is a closed set. For any $\mathbf{a} = (\mathbf{a}_1, \dots, \mathbf{a}_J)^T \in \Omega_i$, we have

$$\|\mathbf{b}_j - \mathbf{a}_j^*\|_2^2 \leq \|\mathbf{b}_j - \mathbf{a}_j\|_2^2, j = 1, 2, \dots, J,$$

so

$$\|\mathbf{b} - \mathbf{a}^*\|_2^2 = \sum_{j=1}^J \|\mathbf{b}_j - \mathbf{a}_j^*\|_2^2 \leq \sum_{j=1}^J \|\mathbf{b}_j - \mathbf{a}_j\|_2^2 = \|\mathbf{b} - \mathbf{a}\|_2^2.$$

That is $\mathbf{a}^* = \arg \min_{\mathbf{a} \in \Omega_i} \|\mathbf{b} - \mathbf{a}\|_2^2$.

On the contrary, let $\mathbf{a}^* = \arg \min_{\mathbf{a} \in \Omega_i} \|\mathbf{b} - \mathbf{a}\|_2^2$. We know that $\mathbf{a}^* \in \Omega_i$ for Ω_i is a closed set. If there exists such an $k \in J$ that $\mathbf{a}_k^* \neq \arg \min_{\mathbf{a}_k \in \Omega_i^{s_j}} \|\mathbf{b}_k - \mathbf{a}_k\|_2^2 \triangleq \mathbf{a}'_k \in \Omega_i^{s_j}$, then $\|\mathbf{b}_k - \mathbf{a}_k^*\|_2^2 > \|\mathbf{b}_k - \mathbf{a}'_k\|_2^2$, we have

$$\|\mathbf{b} - \mathbf{a}^*\|_2^2 > \sum_{j=1, j \neq k}^J \|\mathbf{b}_j - \mathbf{a}_j^*\|_2^2 + \|\mathbf{b}_j - \mathbf{a}'_j\|_2^2 = \|\mathbf{b} - \mathbf{a}'\|_2^2,$$

where $\mathbf{a}' = (\mathbf{a}_1^*, \dots, \mathbf{a}'_k, \dots, \mathbf{a}_J^*) \in \Omega_i$. This is a contradiction to \mathbf{a}^* being the minimum point. \square

Then we design GP algorithm with BB step size for SGCCA problem and its variants as shown in Algorithm 3.

5.2. Convergence analysis for the proposed GP algorithm

To get the convergence of our proposed GP algorithm, we first compute the gradient Lipschitz constant of the objective function $h(\mathbf{a})$. $\forall \mathbf{a}^1 =$

Algorithm 3 The gradient projected algorithm for SGCCA and its variants (SGCCA-GP1, SGCCA-GP1, SGCCA-GP3 corresponding to projection subproblems (P1),(P2) or (P3), respectively)

- 1: Input J blocks $\mathbf{X}_1, \dots, \mathbf{X}_J$, J ℓ_1 constraints s_1, \dots, s_J , a design matrix \mathbf{C} and the scheme, choose J arbitrary normalized vectors $\mathbf{a}_1^0, \mathbf{a}_2^0, \dots, \mathbf{a}_J^0$, initialize the count variable $s = 0$.
- 2: **while** $\|\mathbf{P}_\Omega(\mathbf{a}^s + \gamma_s \nabla h(\mathbf{a}^s)) - \mathbf{a}^s\| \neq 0$ **do**
- 3: set $\mathbf{a}^{s+1} = \mathbf{P}_\Omega(\mathbf{a}^s + \gamma_s \nabla h(\mathbf{a}^s))$, $\mathbf{s}^s = \mathbf{a}^{s+1} - \mathbf{a}^s$;
- 4: for any \mathbf{a}_l^{s+1} , compute

$$\nabla h(\mathbf{a}_l^{s+1}) = \frac{2}{n} \sum_{k=1, k \neq l}^J c_{lk} ((\mathbf{X}_l)^T \mathbf{X}_k \mathbf{a}_k^{s+1})$$

then we can get $\nabla h(\mathbf{a}^{s+1})$, compute $\mathbf{y}^s = \nabla h(\mathbf{a}^{s+1}) - \nabla h(\mathbf{a}^s)$.

- 5: compute $b_s = \langle \mathbf{s}^s, \mathbf{y}^s \rangle$;
 - 6: **if** $b_s \leq 0$ **then**
 - 7: $\gamma_{s+1} = \gamma_{\max}$;
 - 8: **else**
 - 9: compute $\mathbf{a}_s = \langle \mathbf{s}^{(s)}, \mathbf{s}^{(s)} \rangle$;
 - 10: set $\gamma_{s+1} = \min \{ \gamma_{\max}, \max \{ \gamma_{\min}, a_s / b_s \} \}$;
 - 11: **end if**
 - 12: set $s \leftarrow s + 1$;
 - 13: **end while**
-

$$(\mathbf{a}_1^1, \dots, \mathbf{a}_J^1), \mathbf{a}^2 = (\mathbf{a}_1^2, \dots, \mathbf{a}_J^2) \in \mathbb{R}^{p_1} \times \mathbb{R}^{p_2} \dots \times \mathbb{R}^{p_J},$$

$$\begin{aligned} & \|\nabla h(\mathbf{a}^1) - \nabla h(\mathbf{a}^2)\| \\ &= \left\| \begin{pmatrix} \nabla h(\mathbf{a}_1^1) - \nabla h(\mathbf{a}_1^2) \\ \nabla h(\mathbf{a}_2^1) - \nabla h(\mathbf{a}_2^2) \\ \vdots \\ \nabla h(\mathbf{a}_J^1) - \nabla h(\mathbf{a}_J^2) \end{pmatrix} \right\| = \frac{2}{n} \left\| \begin{pmatrix} \sum_{k=2}^J c_{1k} \mathbf{X}_1^T \mathbf{X}_k (\mathbf{a}_k^1 - \mathbf{a}_k^2) \\ \sum_{k=1; k \neq 2}^J c_{2k} \mathbf{X}_2^T \mathbf{X}_k (\mathbf{a}_k^1 - \mathbf{a}_k^2) \\ \vdots \\ \sum_{k=1; k \neq J}^J c_{Jk} \mathbf{X}_J^T \mathbf{X}_k (\mathbf{a}_k^1 - \mathbf{a}_k^2) \end{pmatrix} \right\| \\ &= \frac{2}{n} \sqrt{[\sum_{k=2}^J c_{1k} \mathbf{X}_1^T \mathbf{X}_k (\mathbf{a}_k^1 - \mathbf{a}_k^2)]^2 + [\sum_{k=1, k \neq 2}^J c_{2k} \mathbf{X}_2^T \mathbf{X}_k (\mathbf{a}_k^1 - \mathbf{a}_k^2)]^2 + \dots + [\sum_{k=1, k \neq J}^J c_{Jk} \mathbf{X}_J^T \mathbf{X}_k (\mathbf{a}_k^1 - \mathbf{a}_k^2)]^2} \\ &\leq \frac{2}{n} \sqrt{(J-1) \sum_{k=2}^J [c_{1k} \mathbf{X}_1^T \mathbf{X}_k (\mathbf{a}_k^1 - \mathbf{a}_k^2)]^2 + (J-1) \sum_{k=1, k \neq 2}^J [c_{2k} \mathbf{X}_2^T \mathbf{X}_k (\mathbf{a}_k^1 - \mathbf{a}_k^2)]^2 + (J-1) \sum_{k=1, k \neq J}^J [c_{Jk} \mathbf{X}_J^T \mathbf{X}_k (\mathbf{a}_k^1 - \mathbf{a}_k^2)]^2} \\ &\leq \frac{2}{n} \left(\sqrt{(J-1) \sum_{k=2}^J [c_{1k} \mathbf{X}_1^T \mathbf{X}_k (\mathbf{a}_k^1 - \mathbf{a}_k^2)]^2} + \sqrt{\frac{23}{(J-1) \sum_{k=1, k \neq 2}^J [c_{2k} \mathbf{X}_2^T \mathbf{X}_k (\mathbf{a}_k^1 - \mathbf{a}_k^2)]^2}} + \sqrt{(J-1) \sum_{k=1, k \neq J}^J [c_{Jk} \mathbf{X}_J^T \mathbf{X}_k (\mathbf{a}_k^1 - \mathbf{a}_k^2)]^2} \right) \\ &\leq \frac{2}{n} (\sqrt{J-1} \sum_{k=2}^J \|c_{1k} \mathbf{X}_1^T \mathbf{X}_k (\mathbf{a}_k^1 - \mathbf{a}_k^2)\| + \sqrt{J-1} \sum_{k=1, k \neq 2}^J \|c_{2k} \mathbf{X}_2^T \mathbf{X}_k (\mathbf{a}_k^1 - \mathbf{a}_k^2)\| + \sqrt{J-1} \sum_{k=1, k \neq J}^J \|c_{Jk} \mathbf{X}_J^T \mathbf{X}_k (\mathbf{a}_k^1 - \mathbf{a}_k^2)\|) \\ &\leq \frac{2}{n} (\sqrt{J-1} C \sum_{k=2}^J \|\mathbf{a}_k^1 - \mathbf{a}_k^2\| + \sqrt{J-1} C \sum_{k=1, k \neq 2}^J \|\mathbf{a}_k^1 - \mathbf{a}_k^2\| + \sqrt{J-1} C \sum_{k=1, k \neq J}^J \|\mathbf{a}_k^1 - \mathbf{a}_k^2\|) \end{aligned}$$

where $C = \max_{j \neq k} \|c_{jk} \mathbf{X}_j^T \mathbf{X}_k\|_2$. This shows that $\nabla h(\mathbf{a})$ is Lipschitz continuous with moduli $L_h = \frac{2}{n}(J-1)^{3/2}C\sqrt{J}$.

Now let

$$f_i(\mathbf{a}) = \delta_{\Omega_i}(\mathbf{a}) = \begin{cases} 0, & \mathbf{a} \in \Omega_i \\ +\infty, & \mathbf{a} \notin \Omega_i \end{cases}, \quad i = 1, 2, 3$$

be the indicator function on Ω_i , $i = 1, 2, 3$, and $\Psi_i(\mathbf{a}) = -h(\mathbf{a}) + f_i(\mathbf{a})$, $i = 1, 2, 3$. We will prove $\Psi_i(\mathbf{a})$, $i = 1, 2, 3$ are KL functions. According to the properties of semi-algebraic functions in Bolte et al. (2014), we know that a semi-algebraic function must be a KL function, and the finite sum of semi-algebraic functions is also semi-algebraic. And $h(\mathbf{a}) = \sum_{j,k=1; j \neq k}^J c_{jk} \text{cov}(\mathbf{X}_j \mathbf{a}_j, \mathbf{X}_k \mathbf{a}_k)$ is actually a polynomial function, from Appendix Example 2 in Bolte et al. (2014), we have that $-h(\mathbf{a})$ is a semi-algebraic function. Next we show that $f_i(\mathbf{a}) = \delta_{\Omega_i}(\mathbf{a})$, $i = 1, 2, 3$ are also semi-algebraic functions. However, the indicator function of a semi-algebraic set must be a semi-algebraic function. It has been proved that $\Omega_i^t = \{\mathbf{a}_j : \|\mathbf{a}_j\|_1 \leq t, \|\mathbf{a}_j\|_2 \leq 1\}$, $i = 1, 2, 3; j = 1, 2, \dots, J$ are all semi-algebraic sets in ?. Then Ω_i , $i = 1, 2, 3$ are also semi-algebraic sets. In fact, denote by

$$S_k = \bigcup_{j=1}^p \bigcap_{i=1}^q \{\mathbf{a} \in \mathbb{R}^{p_1+p_2+\dots+p_J} : \|\mathbf{a}_k\|_1 \leq s_k, \|\mathbf{a}_k\|_2 \leq 1\}, k = 1, 2, \dots, J,$$

it is easily verified that $\Omega_i = \Omega_i^{s_1} \times \Omega_i^{s_2} \times \Omega_i^{s_J} = \bigcap_{k=1}^J S_k$ is also a semi-algebraic set. So $\delta_{\Omega_i}(\mathbf{a})$ is semi-algebraic function. Thus $\Psi_i(\mathbf{a})$, $i = 1, 2, 3$ are all KL functions.

Now we can get the convergence result of our proposed SGCCA-GP1, SGCCA-GP2 and SGCCA-GP3 algorithms by Proposition 3 in Bolte et al. (2014) as follows.

Theorem 19. *(Convergence results of the proposed GP algorithm) Let $\{\mathbf{a}^s\}_{s \in \mathbb{N}}$ be a sequence generated by SGCCA-GP1, SGCCA-GP2, or SGCCA-GP3 which is assumed to be bounded and let $\gamma_s > L_h$ computed as above. The following assertions hold:*

(i) The sequence $\{\mathbf{a}^s\}_{s \in \mathbb{N}}$ has finite length, that is,

$$\sum_{s=1}^{\infty} \|\mathbf{a}^{s+1} - \mathbf{a}^s\|_2 < +\infty. \quad (5.4)$$

(ii) The sequence $\{\mathbf{a}^s\}_{s \in \mathbb{N}}$ globally converges to a critical point \mathbf{a}^* of $\Psi_i(\mathbf{a}) = -h(\mathbf{a}) + \delta_{\Omega_i}(\mathbf{a})$, i.e. \mathbf{a}^* satisfies $0 \in \partial\Phi_i$, $i=1, 2$ or 3 .

6. Experiments and results

In order to compare the effectiveness of the improved BCD algorithms SGCCA-BCD1, SGCCA-BCD2 and SGCCA-BCD3 with the original SGCCA algorithm and test the effectiveness of the SGCCA-GP algorithm. we conduct experiments on both artificial data and real glioma data set. All the experients were implemented on R 4.2.0 platform in a PC with 8GB of RAM and an 1.80GHz Intel Core i7-8550U processor under Windows 10.

6.1. Simulations on artificial data

In order to identify active subsets in variable blocks, and show the reliability of the SGCCA algorithm in distinguishing zero and non-zero elements of sparse generalized canonical vectors, according to the way of generating data in Tenenhaus et al. (2014), we consider three variable blocks \mathbf{X}_j , the size of each block is $n \times p_j$, $j = 1, 2, 3$. And they are generated by the following model:

$$\mathbf{X}_j = \mathbf{u}_j \mathbf{w}_j^t + \mathbf{E}_j, j = 1, 2, 3 \quad (6.1)$$

where $\mathbf{u}_1, \mathbf{u}_2, \mathbf{u}_3 \in \mathbb{R}^{50 \times 1}$ follow a multivariate normal distribution with 0 mean and predetermined variance $\text{cov}(\mathbf{u}_1, \mathbf{u}_3) = \text{cov}(\mathbf{u}_2, \mathbf{u}_3) = 0.7$ and $\text{cov}(\mathbf{u}_1, \mathbf{u}_2) = 0$. In addition, $\mathbf{w}_1 \in \mathbb{R}^{200 \times 1}$, $\mathbf{w}_2 \in \mathbb{R}^{500 \times 1}$, $\mathbf{w}_3 \in \mathbb{R}^{700 \times 1}$, only the first 75 elements in $\mathbf{w}_1, \mathbf{w}_2, \mathbf{w}_3$ are nonzero and obey a uniform distribution on $[-0.3, -0.2] \cup [0.2, 0.3]$. $\mathbf{E}_j \in \mathbb{R}^{50 \times p_j}$ is a residual matrix where each element is drawn from a normal distribution with 0 mean and variance equal to 0.2. Since each variable block \mathbf{X}_j and the outer component \mathbf{u}_j are strongly correlated, only the coefficient vector of the first dimension of each block is considered.

6.1.1. Performance indexes

Two quantitative criteria were employed for performance assessment.

Sensitivity: Record the position of the non-zero element in the target variable \mathbf{a}_j , if the element in the corresponding position in \mathbf{w}_j is also nonzero, count the number of such non-zero elements, which is divided by the total number of non-zero elements in \mathbf{w}_j .

Specificity: Record the position of the zero element in the target variable \mathbf{a}_j , if the element in the corresponding position in \mathbf{w}_j is also zero, count the number of zeros, which is divided by the total number of zeros in \mathbf{w}_j .

6.1.2. Results

In this simulations, the design matrix C is defined as $c_{13} = c_{23} = 1, c_{12} = 0$, and the centroid scheme $g(\mathbf{x}) = \mathbf{x}$ are used. And 10000 random initialization of regular vector $\mathbf{a}_1^0, \mathbf{a}_2^0, \mathbf{a}_3^0$ are generated. If we use the BCD algorithms, the ℓ_1 -sparsity parameters are picked respectively as $s_1 = 7.6, s_2 = 8.7$ and $s_3 = 8.05$ by using grid search. If we use the GP algorithms, the ℓ_1 -sparsity parameters are picked respectively as $s_1 = 7.6, s_2 = 8.31$ and $s_3 = 8.05$ by using grid search. Then the 10000 tests are implemented using 7 different algorithms. The following Table ?? shows the sensitivity and specificity.

Table 1: Sensitivity and specificity of different SGCCA algorithms on artificial data using the **Horst** scheme

	sensitivity (mean)			specificity (mean)		
	\mathbf{X}_1	\mathbf{X}_2	\mathbf{X}_3	\mathbf{X}_1	\mathbf{X}_2	\mathbf{X}_3
SGCCA	0.946667	0.853333	0.96	0.952	0.870588	0.976
SGCCA-BCD1	0.946667	0.853333	0.96	0.952	0.870588	0.976
SGCCA-BCD2	0.946667	0.853333	0.96	0.952	0.870588	0.976
SGCCA-BCD3	0.946667	0.853333	0.96	0.952	0.870588	0.976
SGCCA-GP1	0.96	0.853333	0.973333	0.968	0.872941	0.9744
SGCCA-GP2	0.96	0.853333	0.973333	0.968	0.870588	0.9744
SGCCA-GP3	0.96	0.853333	0.973333	0.976	0.872941	0.9744

It can be seen from Table 1 that the sensitivity and specificity of sparse estimation are about 95% for \mathbf{w}_1 and above 95% for \mathbf{w}_3 by using SGCCA algorithm. The SGCCA algorithm is more accurate in selecting the active variable of variable block, but the sparse coefficient vector \mathbf{a}_2 of variable block is less sensitive and accurate, about 85%. For the four algorithms and

each variable block, different initialization vectors have little effect on the changes in sensitivity and specificity.

Furthermore, it can be seen from Table 1 that the proposed algorithms SGCCA-BCD1, SGCCA-BCD2 and SGCCA-BCD3 in this paper can achieve the same solving quality as the original SGCCA algorithm on this artificial data set.

What’s more, the solution quality of SGCCA-GP is higher than SGCCA-BCD.

We further observe the running time of 10,000 experiments of 7 algorithms, and the results are as follows.

Table 2: Comparison of mean time of different SGCCA algorithms on artificial data under 10000 experiments using the **Horst** scheme

	Total Time (min)	Average time(s)	Speedup ratio vs. SGCCA (%)
SGCCA	37.086961	0.222522	-
SGCCA-BCD1	29.448121	0.176689	20.60
SGCCA-BCD2	29.180181	0.17508	21.32
SGCCA-BCD3	31.982509	0.191898	13.76
SGCCA-GP1	91.90446	0.5508	
SGCCA-GP2	94.1508	0.5652	
SGCCA-GP3	106.20354	0.6372	

From Table 2, we also see that the three proposed algorithms SGCCA-BCD1, SGCCA-BCD2 and SGCCA-BCD3 in this paper all have obvious speed acceleration compared with the original SGCCA algorithm. In particular, the average running time of SGCCA-BCD1 algorithm is 0.176689 seconds per experiment, which is 20.6% faster than the original SGCCA algorithm.

In addition, we also see that when using the Horst scheme, GP method takes more time than the original SGCCA algorithm, so it is necessary to make a trade-off between solution quality and solving efficiency.

Furthermore, we also compare the proposed BCD algorithms with the original iterative algorithm when using the centroid scheme $g(\mathbf{x}) = |\mathbf{x}|$ and the factorial scheme $g(\mathbf{x}) = \mathbf{x}^2$. One also sees that our BCD algorithms are also faster than the original SGCCA algorithm with the completely same solution quality. As shown in Table 3-Table 6.

When using the centroid scheme $g(\mathbf{x}) = |\mathbf{x}|$, we select the sparse parameter for a canonical vector as 7.6, 8.6, 8, and obtain the following sensitivity

and specificity.

Table 3: Sensitivity and specificity of different SGCCA algorithms on artificial data using the **centroid** scheme

	sensitivity (mean)			specificity (mean)		
	\mathbf{X}_1	\mathbf{X}_2	\mathbf{X}_3	\mathbf{X}_1	\mathbf{X}_2	\mathbf{X}_3
SGCCA	0.946667	0.853	0.96	0.952	0.877647	0.9776
SGCCA-BCD1	0.946667	0.853	0.96	0.952	0.877647	0.9776
SGCCA-BCD2	0.946667	0.853	0.96	0.952	0.877647	0.9776
SGCCA-BCD3	0.946667	0.853	0.96	0.952	0.877647	0.9776

From Table 3 we can see that the solving qualities of the four algorithms are completely the same when using the centroid scheme. We further test the run time of 10,000 experiments for four algorithms, and the results are as follows.

Table 4: Comparison of mean time of different SGCCA algorithms on artificial data with 10000 experiments using **centroid** scheme

	Total Time (min)	Average time(s)	Speed up ratio vs. SGCCA (%)
SGCCA	25.04966	0.150294	-
SGCCA-BCD1	20.04058	0.120243	19.99
SGCCA-BCD2	21.30313	0.127818	14.95
SGCCA-BCD3	22.37098	0.134226	10.69

From Table 4 it can be seen that when using the centroid scheme, our proposed BCD algorithms SGCCA-BCD1, SGCCA-BCD2 and SGCCA-BCD3 have significant acceleration compared with the original SGCCA algorithm.

When using the factorial scheme $g(\mathbf{x}) = \mathbf{x}^2$, the sparse parameters for the canonical vector are selected as 7.6, 8.31, 8.05, then we get the following results.

Table 5: Sensitivity and specificity of different SGCCA algorithms on artificial data using the **factorial** scheme

	sensitivity (mean)			specificity (mean)		
	\mathbf{X}_1	\mathbf{X}_2	\mathbf{X}_3	\mathbf{X}_1	\mathbf{X}_2	\mathbf{X}_3
SGCCA	0.946667	0.826667	0.96	0.952	0.884706	0.9712
SGCCA-BCD1)	0.946667	0.826667	0.96	0.952	0.884706	0.9712
SGCCA-BCD2	0.946667	0.826667	0.96	0.952	0.884706	0.9712
SGCCA-BCD3	0.946667	0.826667	0.96	0.952	0.884706	0.9712

From Table 5 we can see that the solving qualities of the four algorithms are also completely the same when using the factorial scheme. We also compare the run time of 10,000 experiments for four algorithms, and the results are as follows. From Table 4 we see that when using the factorial scheme, the

Table 6: Comparison of mean time of different SGCCA algorithms in artificial data with 10000 experients using **factorial** scheme

	Total Time (min)	Average time(s)	Speed up ratio vs. SGCCA (%)
SGCCA(factorial)	25.08473	0.15051	
SGCCA-P1(factorial)	18.55881	0.11136	26.01
SGCCA-P2(factorial)	18.30816	0.10986	27.01
SGCCA-P3(factorial)	19.53986	0.11724	22.10

proposed SGCCA-BCD1 , SGCCA-BCD2, SGCCA-BCD3 algorithms have also significant acceleration compared with the original SGCCA algorithm.

6.2. Application to real pediatric glioma data

SGCCA model can be also applied to analyze the possibility of some hypotheses on connections between blocks. One can design the connection matrix C to get the specification of this structural connection between blocks. In this subsection, we further evaluate the performance of the proposed BCD algorithms and GP methods on the real pediatric glioma data set to analyze the 3-block glioma data from different viewpoints like that in Tenenhaus et al. (2014).

6.2.1. Problem and data description

Pediatric high-grade gliomas (pHGG) in different parts present different characteristics in imaging, histology, and prognosis, such as the brainstem,

central nuclei, or supratentorial. Suppose that the genetic origin and carcinogenic pathway of pHGG are related to tumor location. Through comprehensive analysis of gene expression and chromosome imbalance, one can determine more precisely the biological processes and genes that distinguish these pHGG for the different locations.

Glioma dataset consists of pretreatment frozen tumor samples were obtained from 53 children with newly diagnosed pHGG from Necker Enfants Malades (Paris, France) Tenenhaus et al. (2014). The 53 samples are divided into 3 locations: supratentorial (HEMI), central nuclei (MIDL), and brain stem (DIPG). The dataset is organized in 3 blocks of variables: the block \mathbf{X}_1 provides the expression of 15702 genes (GE). The block \mathbf{X}_2 contains the imbalances of 1229 segments (CGH) of chromosomes. The block \mathbf{X}_3 is dummy variables describing the categorical variable location denoted (**loc**) hereafter. Notice that all the variables have been standardized (zero mean and unit variance).

6.2.2. Path diagram

Consider 3 designs for the glioma application:

$$C_1 = \begin{pmatrix} 0, 1, 1 \\ 1, 0, 1 \\ 1, 1, 0 \end{pmatrix} \quad C_2 = \begin{pmatrix} 0, 0, 1 \\ 0, 0, 1 \\ 1, 1, 0 \end{pmatrix} \quad C_3 = \begin{pmatrix} 0, 1, 1 \\ 1, 0, 0 \\ 1, 0, 0 \end{pmatrix} \quad (6.2)$$

where C_1 corresponds to complete connection, C_2 is related to hierarchical connection, and C_3 stands for cascade connection.

Design 1 (C_1) assumes that all blocks are interconnected. SGCCA combined with this design can be used to identify gene (GE) and chromosomal (CGH) variables corresponding to the loss of one allele and the over-expression of the remaining alleles. Design 2 (C_2) is location-oriented prediction, where \mathbf{X}_1 (GE) and \mathbf{X}_2 (CGH) are considered as prediction blocks, and \mathbf{X}_3 represents a response blocks. This design assumes that location-related genes can be identified even if there is no relationship between CGH and GE. Design 3 (C_3) mimics the “central law” in molecular biology which asserts that “DNA makes RNA makes proteins”, and highlights events due to chromosomal imbalances and their consequences for gene expression.

6.2.3. Predictive performance

The location of tumors in the brain is predicted using variable blocks \mathbf{X}_1 (GE) and \mathbf{X}_2 (CGH). To compare the predictive performance of our pro-

posed algorithms SGCCA-BCD1, SGCCA-BCD2 and SGCCA-BCD3 with the original SGCCA algorithm under 3 designs and 3 schemes (total 9 scenarios), a layered 10-pass Monte-Carlo cross validation (MCCV) was used like that in Tenenhaus et al. (2014). For each iteration, randomly selects 9/10 of the data consisting of training set $\mathbf{X}^b = [\mathbf{X}_1^b, \mathbf{X}_2^b, \mathbf{X}_3^b]$, $b = 1, 2, \dots, 10$, and the rest 1/10 data to be the testing set \mathbf{X}^{-b} , we get the sparse generalized canonical vector $\mathbf{a}^b = (\mathbf{a}_1^b, \mathbf{a}_2^b, \mathbf{a}_3^b)$, and the sparse generalized canonical coefficient vector $\mathbf{y}_1^b = \mathbf{X}_1^b \mathbf{a}_1^b$, $\mathbf{y}_2^b = \mathbf{X}_2^b \mathbf{a}_2^b$, $\mathbf{y}_3^b = \mathbf{X}_3^b \mathbf{a}_3^b$ with different algorithms. Estimate the error rate of the testing set in the following three steps:

- (i) Build a Bayesian discriminant model \mathbb{L} of the qualitative variable \mathbf{loc}^b based on the components \mathbf{y}_1^b and \mathbf{y}_2^b ;
- (ii) Compute the sparse generalized canonical vectors $\mathbf{y}_1^{-b} = \mathbf{X}_1^{-b} \mathbf{a}_1^b$ and $\mathbf{y}_2^{-b} = \mathbf{X}_2^{-b} \mathbf{a}_2^b$ of the testing set \mathbf{X}^{-b} ;
- (iii) Predict the labels with \mathbb{L} based on \mathbf{y}_1^{-b} and \mathbf{y}_2^{-b} and compare with the expected labels.

For each MCCV, the sparse parameters are selected using 5-fold cross-validation, and then the parameters with the smallest prediction error are selected.

6.2.4. Experimental results

Fig. 6.1a depicts the boxplot of test error rates on 10 MCCV layers for SGCCA (3 designs, 3 schemes). Fig. 6.1b, 6.1c and 6.1d depicts the boxplot of test error rates on 10 MCCV layers for the proposed algorithms SGCCA-BCD3, SGCCA-BCD1 and SGCCA-BCD2 (3 designs, 3 schemes), respectively.

From Fig. 6.1 one can see that no matter which scheme is used, when using the second design with connection matrix C_2 , the median error rate of is the lowest for all the SGCCA algorithms SGCCA, SGCCA-BCD1, SGCCA-BCD2 and SGCCA-BCD3, which indicates that the structural connection between blocks is location prediction-oriented. According to Fig. 6.1b and Fig. 6.1c, the algorithms SGCCA-BCD1 and SGCCA-BCD3 can get the same solving quality as the original SGCCA algorithm when applied to glioma data, the SGCCA-BCD2 algorithm with connect matrix C_3 and factorial scheme can obtain the same classification error rate as that of the original SGCCA algorithm. However, the classification error rate of the remaining 8 schemes is high and the effect is poor.

We further calculated the running time of four algorithms on glioma data, and the results are as follows.

Observe Table 11, it can be seen that the proposed three algorithms SGCCA-BCD1, SGCCA-BCD2 and SGCCA-BCD3 have obvious speed acceleration compared with the original SGCCA algorithm on glioma data set.

Table 7: The average error rate of four SGCCA-BCD algorithms

glioma	SGCCA-BCD			SGCCA-BCD1		
	Horst	centroid	factorial	Horst	centroid	factorial
Hierarchical	0.2533	0.2533	0.2133	0.253	0.253	0.213
Complete	0.373	0.45	0.47	0.37	0.45	0.47
Cascade	0.47	0.397	0.47	0.47	0.397	0.47
glioma	SGCCA-BCD2			SGCCA-BCD3		
	Horst	centroid	factorial	Horst	centroid	factorial
Hierarchical	0.23	0.23	0.287	0.253	0.253	0.213
Complete	0.45	0.487	0.53	0.37	0.45	0.47
Cascade	0.49	0.47	0.47	0.47	0.397	0.47

Table 8: The running time of different SGCCA-BCD algorithms on glioma data

glioma	Total time(hour)	Speed up ratio vs. SGCCA(%)
SGCCA	36.936648	-
SGCCA-BCD1	22.79036	38.30
SGCCA-BCD2	18.11889	50.95
SGCCA-BCD3	22.85714	38.12

Next, we test the GP method with the Horst scheme $g(\mathbf{x}) = \mathbf{x}$, and the results are as follows. Then we calculated the average error rate of the four algorithms. It can be seen that the average error rate of SGCCA-GP is significantly lower than that of the original SGCCA algorithm, and the error rate using hierarchical matrix is the lowest, indicating that the variable blocks are more position-oriented prediction, emphasizing the appearance of tumors caused by gene expression and chromosome deletion in different locations.

We also compare the running time of our GP algorithms with the original SGCCA algorithm, the results are shown in Table 13.

From Table 13 we can see that for high-dimensional data, the solving time of our GP algorithm is a little longer than that of the original SGCCA algorithm.

Table 9: The running time of different SGCCA-BCD algorithms on glioma data using the Horst scheme

glioma	Total time(hour)	Speed up ratio vs. SGCCA(%)
SGCCA	12.39054	-
SGCCA-BCD1	7.911448	36.15
SGCCA-BCD2	6.027227	51.36
SGCCA-BCD3	7.971956	35.66

Table 10: The running time of different SGCCA-BCD algorithms on glioma data using the centroid scheme

glioma	Total time(hour)	Speed up ratio vs. SGCCA(%)
SGCCA	12.56542	-
SGCCA-BCD1	8.19548	34.78
SGCCA-BCD2	6.102885	51.43
SGCCA-BCD3	8.152752	35.12

Table 11: The running time of different SGCCA-BCD algorithms on glioma data using the factorial scheme

glioma	Total time(hour)	Speed up ratio vs. SGCCA(%)
SGCCA	12.85489	-
SGCCA-BCD1	8.528464	33.66
SGCCA-BCD2	6.620811	48.50
SGCCA-BCD3	8.53202	33.63

7. Conclusions and future work

In this paper, we first characterize the solution to the linear function maximization subproblems LM-P1, LM-P2 and LM-P3 on the intersection of an ℓ_1 -norm ball and a unit ℓ_2 -norm ball, an ℓ_1 -norm sphere and a unit ℓ_2 -norm sphere and an ℓ_1 -norm ball and a unit ℓ_2 -norm sphere, respectively. Then we provide more efficient BCD algorithms for SGCCA and its two variants, prove that they all globally converge to their stationary points. We further propose gradient projected (GP) methods for SGCCA and its two variants when using the Horst scheme, and prove that they all globally converge to their critical points. Finally, we conduct two numerical experiments in R environment to evaluate the performance of our proposed BCD algorithms and GP methods for SGCCA and its variants. Simulation results show that with the same solution quality, our BCD algorithms are more faster than the original SGCCA algorithm; our GP methods improve the solution quality with a little bit lost efficiency on the artificial data, improve the solution quality and efficiency on the real glioma data using the Horst scheme. In the future, the (sub)gradient method may be considered for SGCCA when using the centroid scheme or factorial scheme.

Table 12: The average error rate of four SGCCA algorithms using the **Horst** scheme

glioma	SGCCA	SGCCA-GP1	SGCCA-GP2	SGCCA-GP3
Hierarchical	0.253333	0.243333	0.296667	0.296667
Complete	0.373333	0.323333	0.303333	0.303333
Cascade	0.47	0.28	0.263333	0.263333

Table 13: The running time of four SGCCA algorithms on glioma data using the **Horst** scheme

glioma	Total time(hour)	Speed up ratio vs. SGCCA(%)
SGCCA	12.58325	-
SGCCA-GP1	16.84279	-
SGCCA-GP2	13.26407	-
SGCCA-GP3	13.3175	-

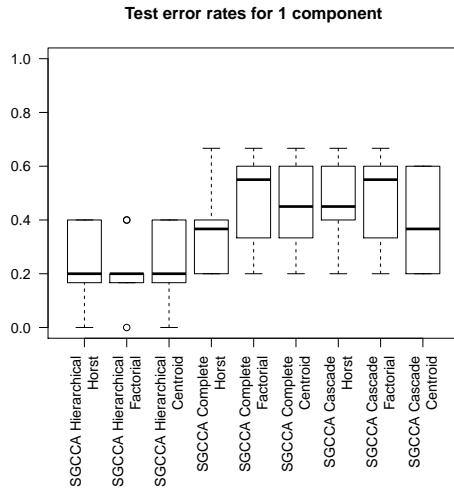
Acknowledgement

We would like to express our gratitude to Associate Professor Hongying Liu for her kind help and useful recommendations.

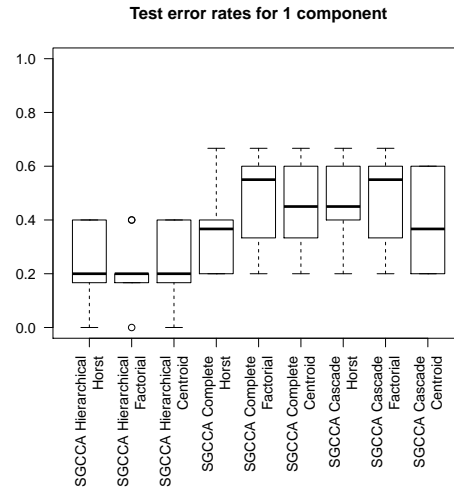
References

- A. Tenenhaus, C. Philippe, V. Guillemot, K.-A. Le Cao, J. Grill, V. Frouin, Variable Selection for Generalized Canonical Correlation Analysis., *Biostatistics* 15 (3) (2014) 569–583, ISSN 1465-4644, doi:10.1093/biostatistics/kxu001, URL <https://doi.org/10.1093/biostatistics/kxu001>.
- D. M. Witten, R. Tibshirani, T. Hastie, A Penalized Matrix Decomposition, with Applications to Sparse Principal Components and Canonical Correlation Analysis, *Biostatistics Oxford, England* 10 (3) (2009) 515–534, ISSN 1465-4644, doi: 10.1093/biostatistics/kxp008.
- H. Hotelling, Relations Between Two Sets of Variates, *Biometrika* 28 (3-4) (1936) 321–377, ISSN 0006-3444, doi:10.1093/biomet/28.3-4.321, URL <https://doi.org/10.1093/biomet/28.3-4.321>.
- P. Horst, Relations among m sets of measures, *Psychometrika* 26 (1961) 129–149.
- J. R. Kettenring, Canonical analysis of several sets of variables, *Biometrika* 58 (1971) 433–451.
- D. Torres, D. Turnbull, L. Barrington, G. Lanckriet, Identifying Words that are Musically Meaningful,, *Austrain Computer Society*, 405–410, 2007.
- M. Hanafi, PLS Path Modelling: Computation of Latent Variables with the Estimation Mode B, *Comput. Stat.* 22 (2) (2007) 275–292, ISSN 0943-4062.
- H. Liu, H. Wang, M. Song, Projections onto the Intersection of a One-Norm Ball or Sphere and a Two-Norm Ball or Sphere, *Journal of Optimization Theory and Applications* 187 (2020) 520–534.

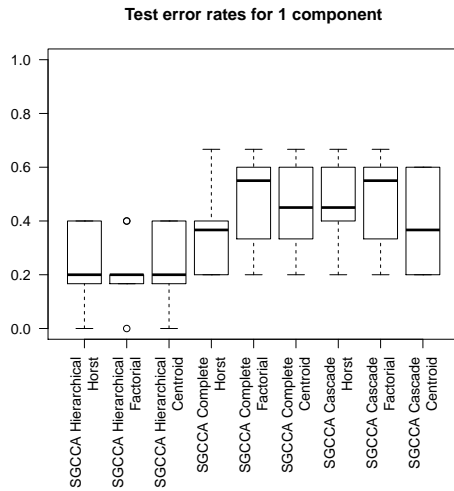
- Q. Zhao, D. Meng, Z. Xu, C. Gao, A block coordinate descent approach for sparse principal component analysis, *Neurocomputing* 153 (2015) 180–190, ISSN 0925-2312, doi:<https://doi.org/10.1016/j.neucom.2014.11.038>, URL <https://www.sciencedirect.com/science/article/pii/S0925231214015719>.
- P. Tseng, Convergence of a Block Coordinate Descent Method for Nondifferentiable Minimization, *Journal of Optimization Theory and Applications* 109 (2001) 475–494, doi: [10.1023/A:1017501703105](https://doi.org/10.1023/A:1017501703105).
- J. Bolte, S. Sabach, M. Teboulle, Proximal alternating linearized minimization for non-convex and nonsmooth problems, *Mathematical Programming* 146 (2014) 459–494, doi: [10.1007/s10107-013-0701-9](https://doi.org/10.1007/s10107-013-0701-9).



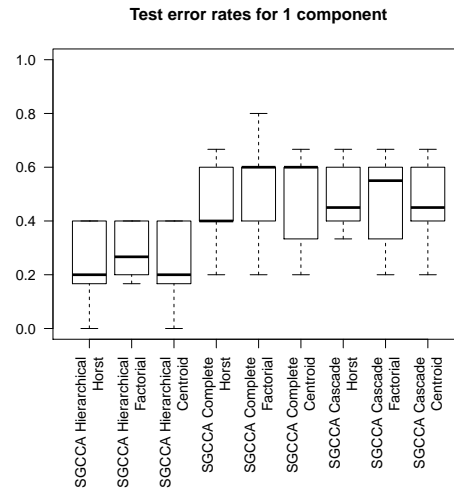
(a) Test error rates of the original SGCCA algorithm for glioma data



(b) Test error rates of the SGCCA-BCD3 algorithm for glioma data

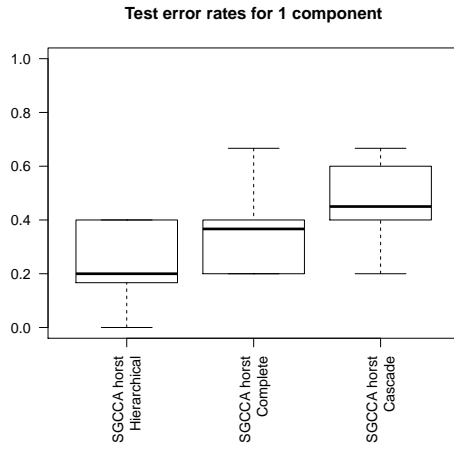


(c) Test error rates of the SGCCA-BCD1 algorithm for glioma data

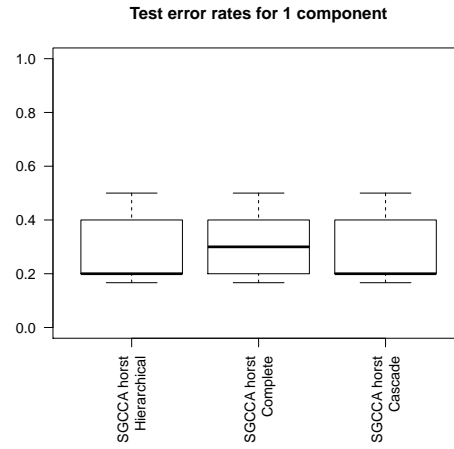


(d) Test error rates of the SGCCA-BCD2 algorithm for glioma data

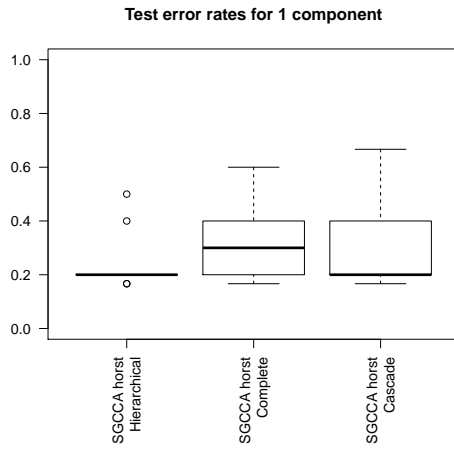
Figure 6.1: The classification error rate of glioma data using the original SGCCA algorithm and the proposed algorithms SGCCA-BCD1, SGCCA-BCD2 and SGCCA-BCD3.



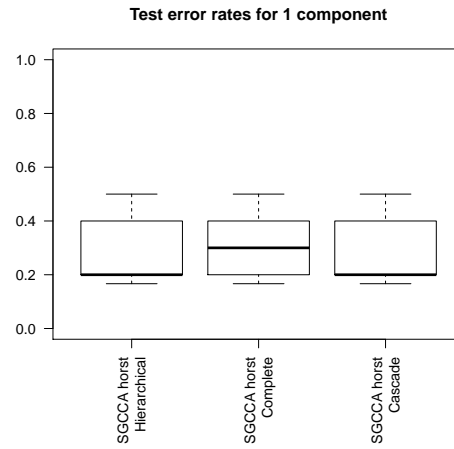
(a) Test the original SGCCA algorithm for glioma data



(b) Test the SGCCA-GP3 algorithm for glioma data



(c) Test the SGCCA-GP1 algorithm for glioma data



(d) Test the SGCCA-GP2 algorithm for glioma data

Figure 6.2: The classification error rate of glioma data using the proposed algorithms SGCCA-GP1, SGCCA-GP2 and SGCCA-P3.